

Ash Dispersal Forecast and Civil Aviation Workshop

Geneva, Switzerland, 18-20 October 2010

Hekla 2000 Benchmark Document

Costanza Bonadonna¹, Arnau Folch², Susan Loughlin³, Herbert Puempel⁴

¹Earth and Environmental Sciences Section, University of Geneva, Switzerland

²Barcelona Supercomputing Center, Spain

³British Geological Survey, U.K.

⁴World Meteorological Organization, Switzerland

Contributors:

Barsotti, S.¹, Biass S.², Costa, A.³, Dellinger, R.⁴, D'Amours, R.⁵, Graf, H.⁶, Herzog, M.⁶, Hort, M.⁷, Kristiansen, N.⁸, Macedonio, G.³, Malo, A.⁵, Martet, M.⁹, Mastin, L.⁴, Neri, A.¹, Peuch, A.⁹, Shimbori, T.¹⁰, Stunder, B.¹¹, Webley, P.¹²

¹Istituto Nazionale di Geofisica e Vulcanologia, Sezione di Pisa, Italy

²Earth and Environmental Sciences Section, University of Geneva, Switzerland

³Istituto Nazionale di Geofisica e Vulcanologia, Sezione di Napoli, Italy

⁴USGS, Cascades Volcano Observatory, USA

⁵Canadian Meteorological Centre, Canada

⁶Department of Geography, University of Cambridge, UK

⁷Meteorological Office, London VAAC, UK

⁸Norwegian Institute for Air Research, Norway

⁹Volcanic Ash Advisory Centre, Météo France, Toulouse, France

¹⁰Meteorological Research Institute, JMA, Japan

¹¹NOAA Air Resources Laboratory, USA

¹²Geophysical Institute, University of Alaska Fairbanks, USA

Citation: Bonadonna, C, Folch, A, Loughlin, S, Puempel, H (2011), "Ash Dispersal Forecast and Civil Aviation Workshop - Model Benchmark Document," <https://vhub.org/resources/505>

Contents

1. Objective	3
2. Summary of the eruption chronology	3
3. Definition of the benchmark	4
3.1. Eruption characteristics (explosive phase)	4
3.2. Granulometry and particle density	4
3.3. Meteorological data	5
3.4. Configuration of models and comments	5
4. Results	8
5. References	8
Plate 1. Concentration contours at 27 FEB 2000, 00:20UTC (6h)	
Plate 1.a. Values at FL100	9
Plate 1.b. Values at FL200	11
Plate 1.c. Values at FL300	13
Plate 2. Concentration contours at 27 FEB 2000, 12:20UTC (18h)	
Plate 2.a. Values at FL100	15
Plate 2.b. Values at FL200	17
Plate 2.c. Values at FL300	19
Plate 3. Concentration contours at 28 FEB 2000, 00:20UTC (30h)	
Plate 3.a. Values at FL100	21
Plate 3.b. Values at FL200	23
Plate 3.c. Values at FL300	25
Plate 4. Concentration contours at 28 FEB 2000, 12:20UTC (42h)	
Plate 4.a. Values at FL100	27
Plate 4.b. Values at FL200	29
Plate 4.c. Values at FL300	31
Plate 5. Concentration contours at 29 FEB 2000, 00:20UTC (54h)	
Plate 5.a. Values at FL100	33
Plate 5.b. Values at FL200	35
Plate 5.c. Values at FL300	37
Plate 6. Concentration contours at 29 FEB 2000, 12:20UTC (66h)	
Plate 6.a. Values at FL100	39
Plate 6.b. Values at FL200	41
Plate 6.c. Values at FL300	43
Plate 7. Vertical concentration profiles at point (5°W,75°N)	
Plate 7.a. Values at 27 FEB 2000, 23:20UTC (29h)	45
Plate 7.b. Values at 28 FEB 2000, 01:20UTC (31h)	47
Plate 7.c. Values at 28 FEB 2000, 03:20UTC (33h)	49
Plate 7.d. Values at 28 FEB 2000, 05:20UTC (35h)	51
Plate 7.e. Values at 28 FEB 2000, 07:20UTC (37h)	53
Plate 7.f. Values at 28 FEB 2000, 09:20UTC (39h)	55
Plate 7.g. Values at 28 FEB 2000, 11:20UTC (41h)	57
Plate 8. Ground deposit load	59
Plate 9. Ground deposit load at different distances from the vent	61

1. Objective

One of the main objectives of the “Ash dispersal forecast and civil aviation” workshop was to investigate the state of existing Volcanic Ash Transport and Dispersal Models (VATDM) in order to identify potential new improved strategies of dispersal forecasting, e.g. probability/ensemble forecasting. In this context, a benchmark case (26 Feb. 2000 Hekla eruption) was run using different state-of-the-art Volcanic Ash Transport and Dispersion Models (VATDM) to understand better the variability associated with different modelling approaches when using the same (or very similar) input dataset.

2. Summary of the eruption chronology

Hekla began erupting at 18:19 (LT=UTC) on February 26th 2000. Precursory earthquake activity was noted at 17:00, with small earthquakes detected by a seismograph close to the summit of the volcano followed by larger earthquakes at 17:29. Continuous low-frequency tremor began at the same time when the eruption cloud was first observed, indicating the start of the explosive phase of the eruption at 18:19 (<http://www.earthice.hi.is/page/hekla26feb2000>).

A more than 10 km high eruption column formed in the first few minutes of the eruption reaching a maximum of 12.5km, detected by radar in Keflavík and observed by aircraft and from the ground (Höskuldsson et al. 2007). Weather conditions were poor and the eruption started in darkness so that direct visual observations of the early part of the eruption are limited (Höskuldsson et al. 2007). Radar observations are discussed at Lacasse et al. (2004) and satellite observations at Rose et al. (2003). The explosive part of the eruption lasted only a short time, around 60 minutes, reaching a peak after only 40 minutes after which time a fissure of 6.6km length began to open (Höskuldsson et al. 2007).

Tephra fall was deposited mainly during the most explosive phase when the plume was carried approximately northwards by the prevailing wind. Tephra fall reached Grímsey after 3 hours and covered an area of approximately 18,000 km³ (Haraldsson 2001, Haraldsson et al 2002). On the second day wind changed direction depositing small amounts of tephra to the south of Hekla (Haraldsson 2001, Haraldsson et al 2002). The explosive phase of the eruption was followed by fire fountaining and strombolian activity, neither of which produced significant tephra fall. The majority of the mass erupted in the Hekla 2000 eruption formed lava flows that flowed generally to the south from the Hekla ridge. The last eruptive production was observed on March 5th 2000 and the last eruptive tremor was detected on 8th March 2000. The eruption lasted 11 days (<http://www.earthice.hi.is/page/hekla4-8mars2000>). More detailed chronology can be found at the Icelandic Institute of Earth Sciences web page: http://www.earthice.hi.is/page/ies_hekla2000

3. Definition of the benchmark

The benchmark exercise considered 12 VATDM (in alphabetical order):

- 1) ASH3D
- 2) ATHAM
- 3) FALL3D
- 4) FLEXPART
- 5) HYSPLIT
- 6) JMA
- 7) MLDP0
- 8) MOCAGE
- 9) NAME
- 10) PUFF
- 11) TEPHRA2
- 12) VOL-CALPUFF

Details of these models can be found in the companion *Model definition* document.

3.1. Eruption characteristics

The Table below summarizes the characteristics of the explosive phase of the Hekla 2000 eruption.

<i>Vent coordinates</i>	lat-lon (63.98°N, 19.67°W) UTM (zone 27) (565000, 7096500)
<i>Vent height (a.s.l.)</i>	1.5 km
<i>Eruption phase start</i>	26 FEB 2000 at 18:20 UTC
<i>Eruption phase end</i>	26 FEB 2000 at 19:30 UTC
<i>Duration</i>	1h 10 min
<i>Column height (above vent)</i>	12.0 km (13.5 km a.s.l.)
<i>Total erupted mass (tephra)</i>	2.0×10^{10} kg
<i>Average mass eruption rate</i>	4.8×10^6 kg/s
<i>Deposit density</i>	611 kg/m^3
<i>Erupted SO₂ mass</i>	2.0×10^8 kg
<i>Erupted mass of fine ash (< 63 μm)</i>	$\approx 0.5\text{-}1 \times 10^9$ kg

Table 1. Eruption characteristics

3.2. Granulometry and particle density

Granulometry and particle density were available for 16 grain-size classes ranging from 32 mm ($\phi=-5$) to 1 μ m ($\phi=10$) (from Smith et al. in preparation). Table 2 gives weight fraction and density for each size class. Models that are less flexible in the number of size classes and/or particle size ran the simulation with a different granulometric discretization but, in this case, the erupted mass was scaled accordingly (see section 3.4).

ϕ	diameter (mm)	weight fraction (%)	density (kg/m ³)
-5	32	0.04	513.00
-4	16	6.34	513.00
-3	8	15.59	513.00
-2	4	11.91	513.00
-1	2	6.83	513.00
0	1	4.59	773.88
1	0.5	2.15	1034.76
2	0.25	6.97	1295.64
3	0.125	22.22	1556.52
4	0.0625	20.85	1817.40
5	0.03125	1.69	2078.28
6	0.015625	0.46	2339.16
7	0.0078125	0.13	2600.00
8	0.00390625	0.11	2600.00
9	0.001953125	0.09	2600.00
10	0.000976563	0.04	2600.00

Table 2. Total Grain Size Distribution (TGSD) and densities

3.3 Meteorological data

Wind field is a necessary input for any VATDM. Most models also require additional meteorological variables such as temperature or air density. Standardization of meteorological data is not a trivial issue for a number of reasons (e.g. some models admit certain inputs only, other run coupled with a specific Numerical Weather Prediction Model, etc.). For benchmarking purposes three types of meteorological datasets were furnished (to be used in order of preference):

1. ECMWF ERA-40 reanalysis (interpolated at 0.25° resolution)
2. NCEP/NCAR reanalysis-1 data (at 2.5° resolution)
3. Vertical wind profiles above the vent

3.4. Configuration of models and comments

3.4.1. ASH3D

Eruption characteristics: as in Table 1
 Grain size distribution: as in Table 2
 Source term: Suzuki distribution with k=4
 Terminal velocities: Wilson and Huang (1979) with F=0.4
 Vertical discretization: 1km
 Horizontal discretization: 0.1° (regional domain) and 0.02° (local domain).

3.4.2. ATHAM

ATHAM is a plume model. For computational limitations, only 6h of simulations in the small domain were performed.

3.4.3. FALL3D

Eruption characteristics:	as in Table 1
Grain size distribution:	as in Table 2
Source term:	Suzuki distribution with $A=4$ and $\lambda=1$
Terminal velocities:	Ganser (1993)
Vertical discretization:	0.2km
Horizontal discretization:	0.25° (regional domain) and 3km (local domain).

3.4.4. FLEXPART

Eruption characteristics:	as in Table 1
Grain size distribution:	as in Table 2
Source term:	Uniformly distributed between 1.5 and 12 km a.s.l.
Model output:	1 hour average concentrations Large Domain: Grid resolution: 0.25° x 0.25° Small Domain: Grid resolution: 0.05° x 0.05° Vertical resolution: 250 meters
Flight level definitions	Exact flight levels are not used. Concentration at FLXXX is the average concentrations over height level $FLXXX \pm 025$ ($FL \approx FL \pm 760$ m).

3.4.5. HYSPLIT

Eruption characteristics:	as in Table 1
Grain size distribution:	8 particle size bins, from 1 to 125 μm (10 to 3Φ).
Source term:	Vertical line source
Model output:	6 hour average concentrations

3.4.6. JMA

The JMA Global Tracer Transport Model for volcanic ash is now under development and will be operational at Tokyo VAAC in 2012. Meteorological data used is 3-hour outputs of the total 84-hour forecast of the JMA-GSM from the initial 1200UTC 26 Feb. 2000 provided by the JRA-25.

Eruption characteristics:	as in Table 1
Grain size distribution:	Upper limit is 0.25 mm (from $\phi=2$ to 10).
Source term:	Uniformly distributed between 1.5 and 12 km a.s.l.
Terminal velocities:	Suzuki (1983) with $F=0.43$
Model output:	Airborne concentration at the valid time instant.
Large Domain:	Grid resolution: 1 degree x 1 degree
Vertical resolution:	1000 ft

3.4.7. MLDP0

Eruption characteristics:	as in Table 1
Grain size distribution:	Model not adapted to variations of particle densities. Ran 4 different simulations using different values of the particle density.
Source term:	Uniformly distributed between 1.5 and 12 km Horizontal dispersion source radius: 1 km

Model output: 20min average concentrations
Large Domain: Grid resolution: 25 km at 60°N
Small Domain: Grid resolution: 5 km at 60°N
Flight level definitions Concentration at FLXXX is the average concentrations
over height level FLXXX ± 050

3.4.8. MOCAGE

Eruption characteristics: as in Table 1
Grain size distribution: as in Table 2
Source term: Uniformly distributed between 1.5 and 12 km a.v.
Vertical discretization: 47 levels
Horizontal discretization: 0.25°

3.4.9. NAME

Eruption characteristics: as in Table 1
Grain size distribution: as in Table 2
Source term: Uniformly distributed between 1.5 and 12 km a.s.l.
Model output: 1 hour average concentrations
Large Domain: Grid resolution: 0.2° x 0.1°
Small Domain: Grid resolution: 0.1° x 0.05°
Flight level definitions Exact flight levels are used.
Concentration at FLXXX is the average concentrations
over height level FLXXX ± 025.

3.4.10. PUFF

Not provided

3.4.11. TEPHRA2

Eruption characteristics: as in Table 1
Grain size distribution: as in Table 2
Source term: Uniform distribution, step 200m
Model output: Only ground deposit.

3.4.12. VOLCALPUFF

Not provided

4. Results

The model comparison was based on the following outputs:

- 1) Maps of airborne concentration. Selected maps are shown in Plates 1 to 6 (FL100, FL200 and FL300 every 12 hours). The full collection of maps is available on the workshop website (i.e. FL100, FL200, FL300 and FL350 every 6 hours): <http://www.unige.ch/sciences/terre/mineral/CERG/Workshop.html>
- 2) Vertical profiles of concentration at the point of coordinates (5°W,75°N) at different time instants (Plate 7).
- 3) Maps of ground deposit load (Plate 8).
- 4) Plot of the deposit load at different distances from the vent (Plate 9).

5. References

- Haraldsson, K. Ö. 2001. Heklugosið 2000, dreifing gjósku frá fyrsta gosdegi á landi. *B.S. Thesis*, Institute of Earth Sciences, University of Iceland. (in Icelandic).
- Haraldsson, K. Ö, Árnasson, S. G., Larsen, G., Eiríksson, J. 2002. The Hekla eruption of 2000 – The tephra fall. *25th Nordic Geological Winter Meeting, Reykjavík, Abstract*.
- Höskuldsson, Á, N. Óskarsson, R. Pedersen, K.Grönvold, K. Vogfjörð and R. Ólafsdóttir 2007. The millennium eruption of Hekla in February 2000, *Bulletin of Volcanology*, Volume 70, Number 2
- Ganser, G. (1993), A rational approach to drag prediction of spherical and nonspherical particles. *Powder Technology* 77, 143–152.
- Lacasse, C., S. Karlsdóttir, G. Larsen, H. Soosalu, W. I. Rose and G. G. J. Ernst 2004. Weather radar observations of the Hekla 2000 eruption cloud, Iceland, *Bulletin of Volcanology*, 66, 457-473.
- Smith KT, C. Bonadonna, Á. Höskuldsson¹, G. Larsen¹, F. Sigmundsson (in prep.), New physical constraints of the 2000 Hekla eruption.
- Suzuki, T. 1983. A theoretical model for dispersion of tephra. :Arc volcanism: Physics and tectonics, D. Shimozuru and I. Yokoyama, editors, TERRAPUB, Tokyo, pp. 95-113.
- Wilson, L., and Huang, T.C., 1979, The influence of shape on the atmospheric settling velocity of volcanic ash particles, *Earth and Planetary Science Letters*, v. 44, pp. 311-324.



Plate 1.a

Concentration contours at FL100 (27 FEB 2000, 00:20UTC, 6h).

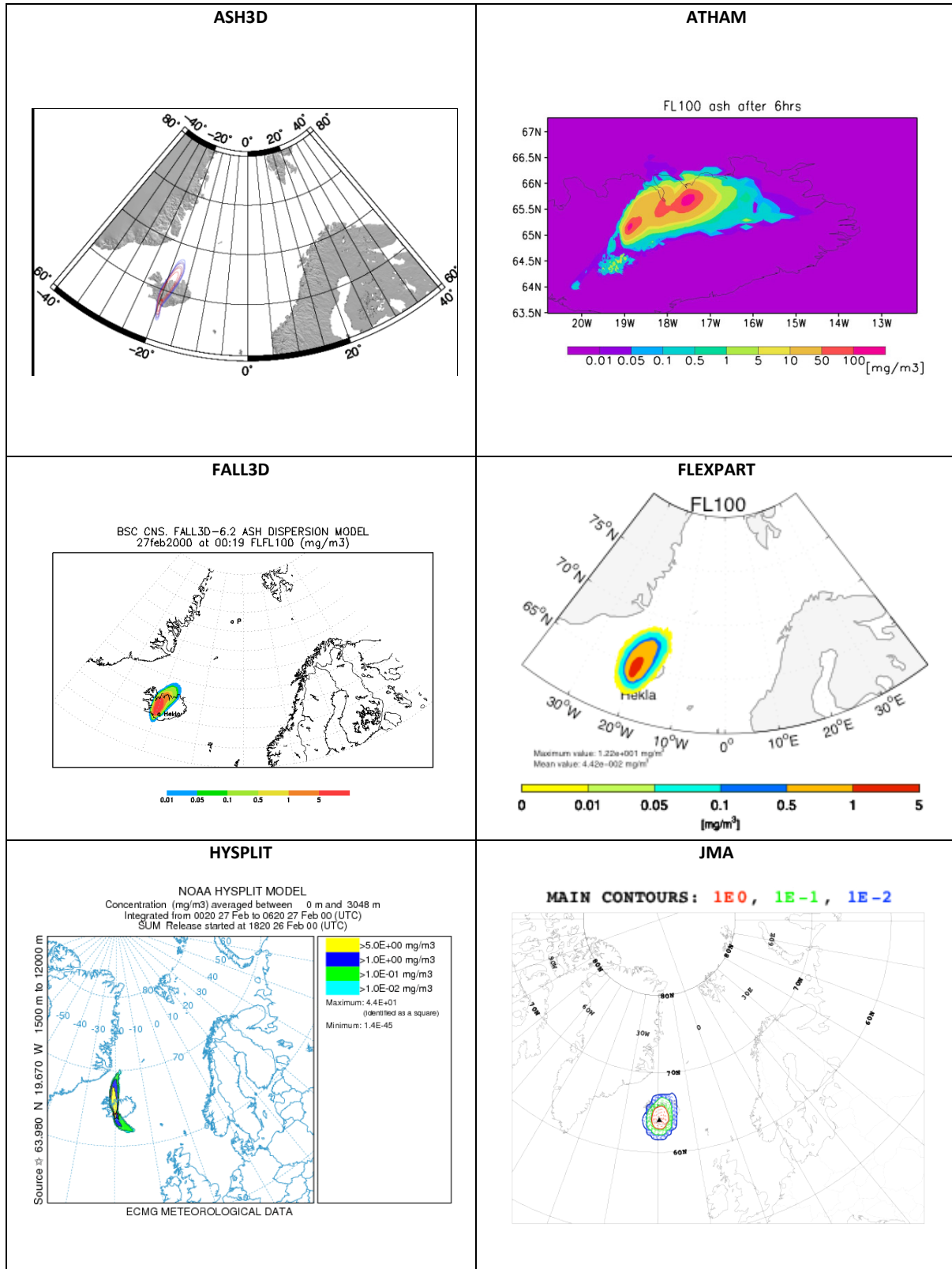


Plate 1.a (cont.)

Concentration contours at FL100 (27 FEB 2000, 00:20UTC, 6h).

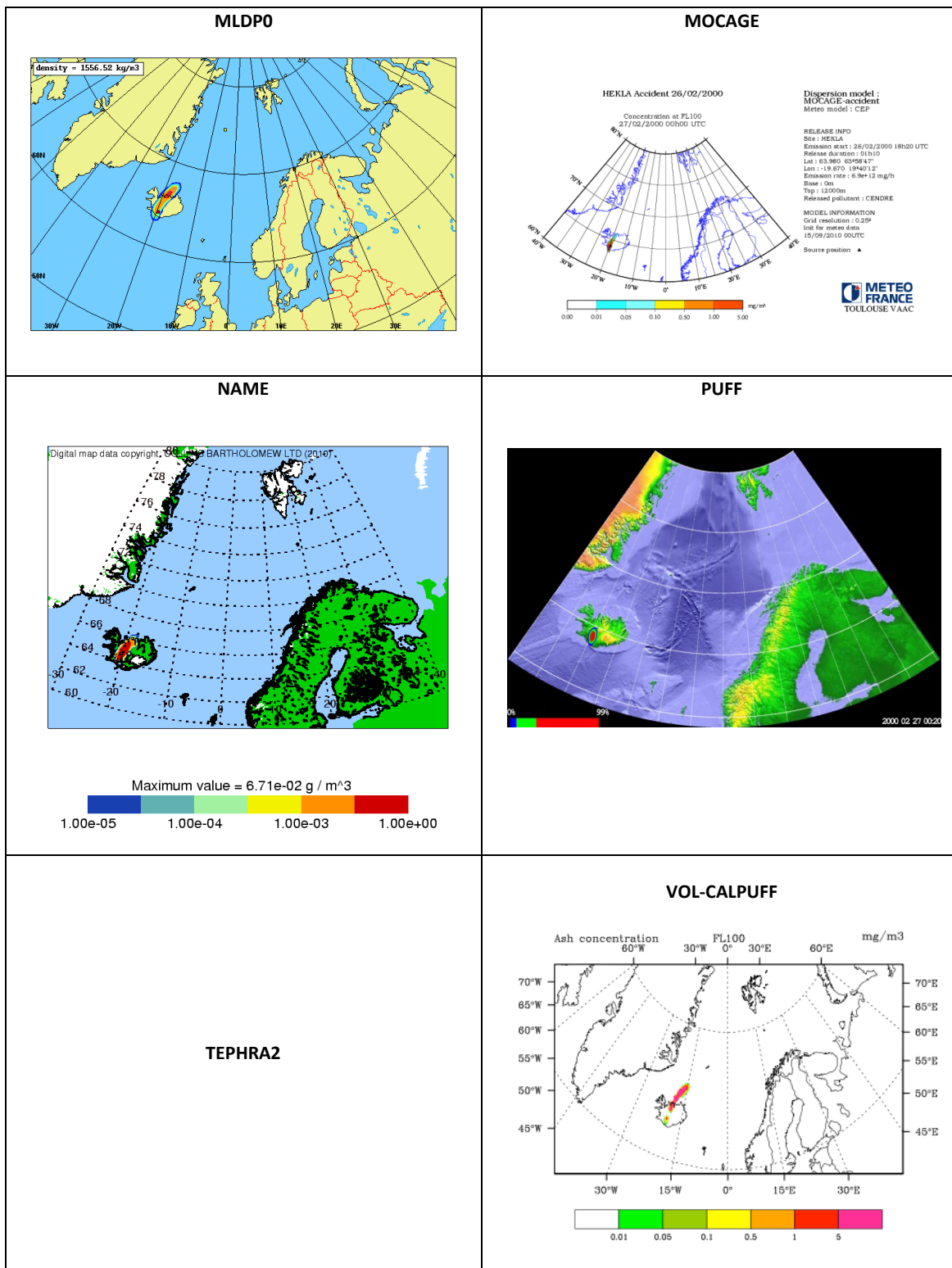




Plate 1.b

Concentration contours at FL200 (27 FEB 2000, 00:20UTC, 6h).

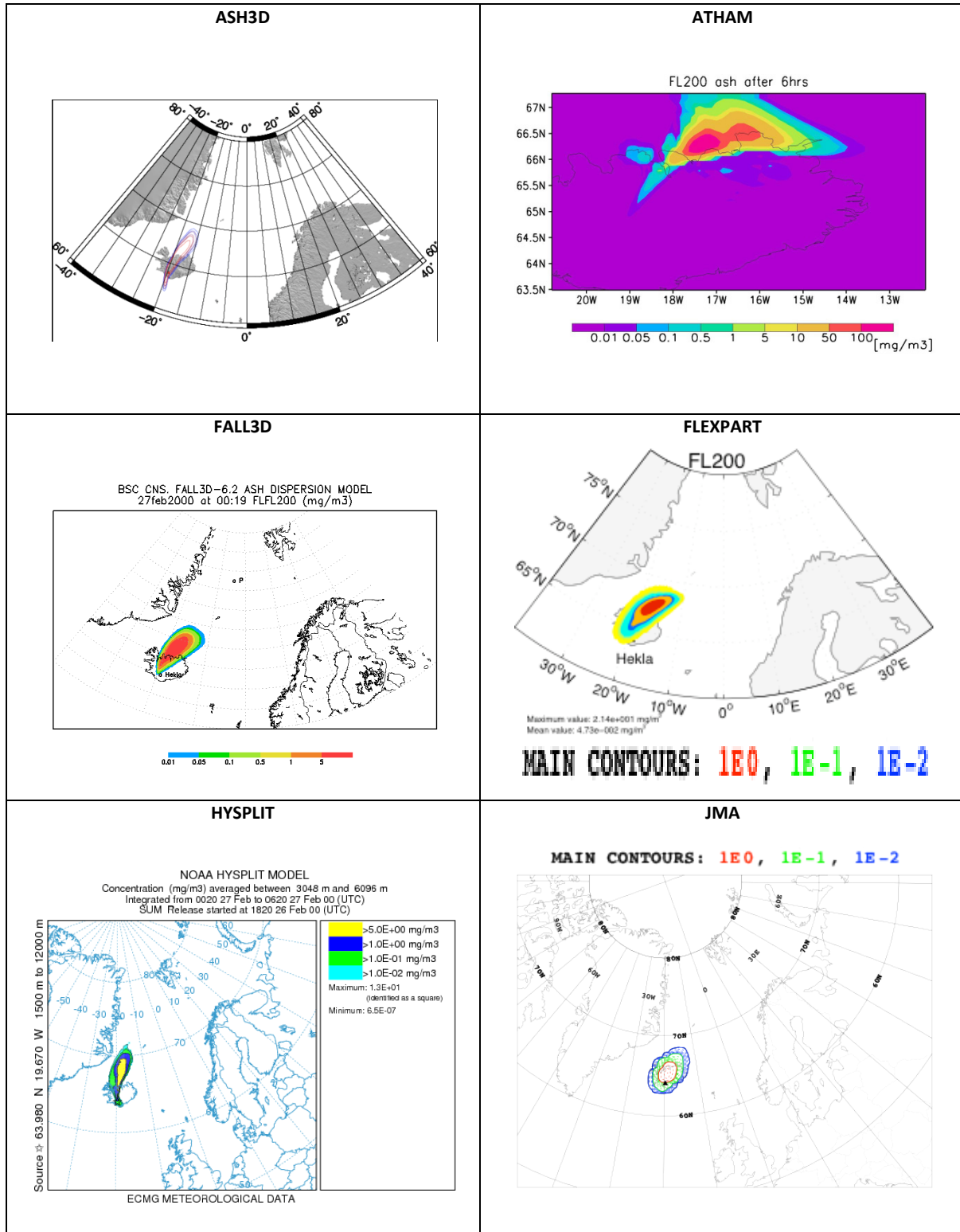


Plate 1.b (cont.)

Concentration contours at FL200 (27 FEB 2000, 00:20UTC, 6h).

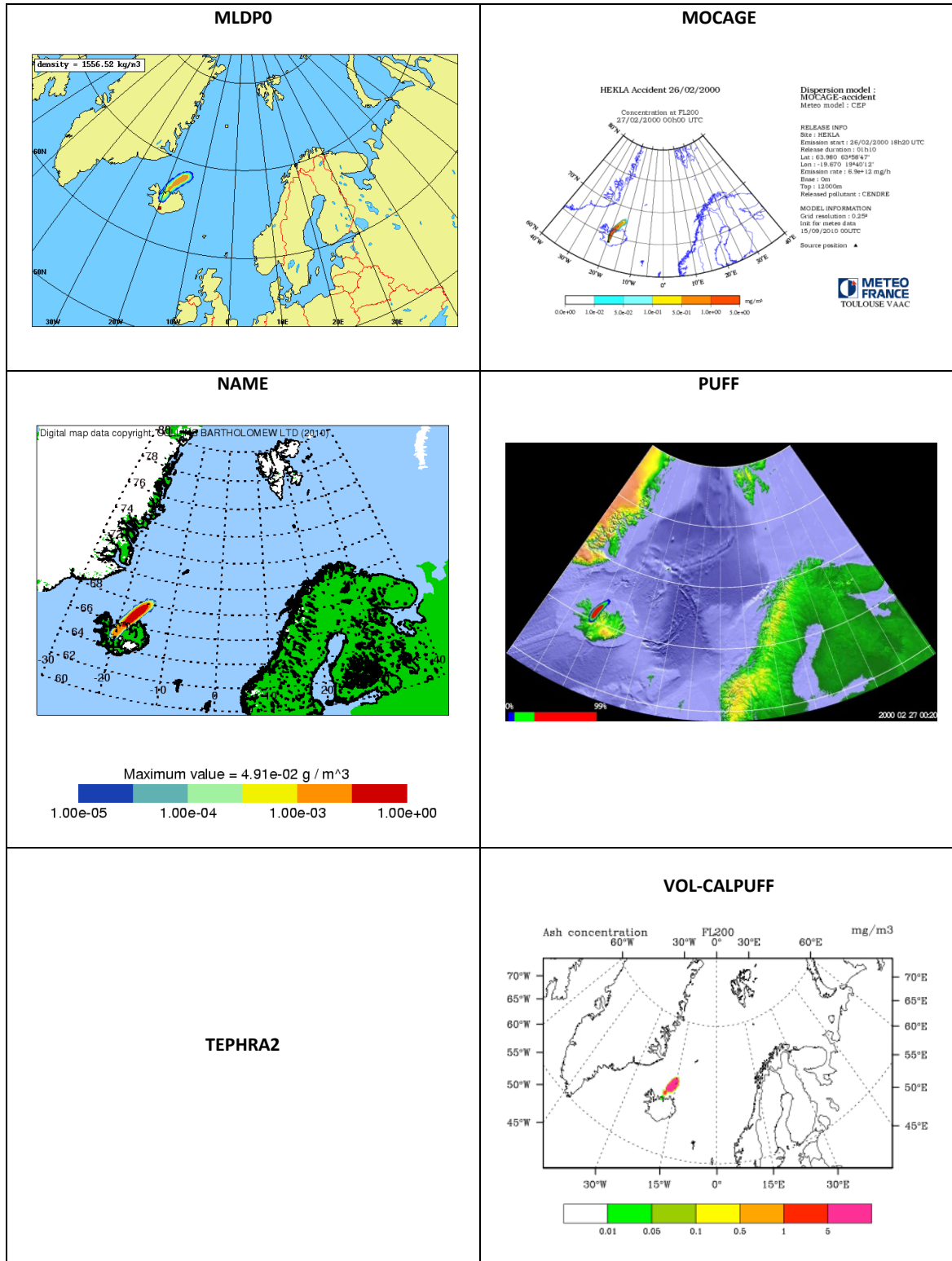


Plate 1.c
Concentration contours at FL300 (27 FEB 2000, 00:20UTC, 6h).

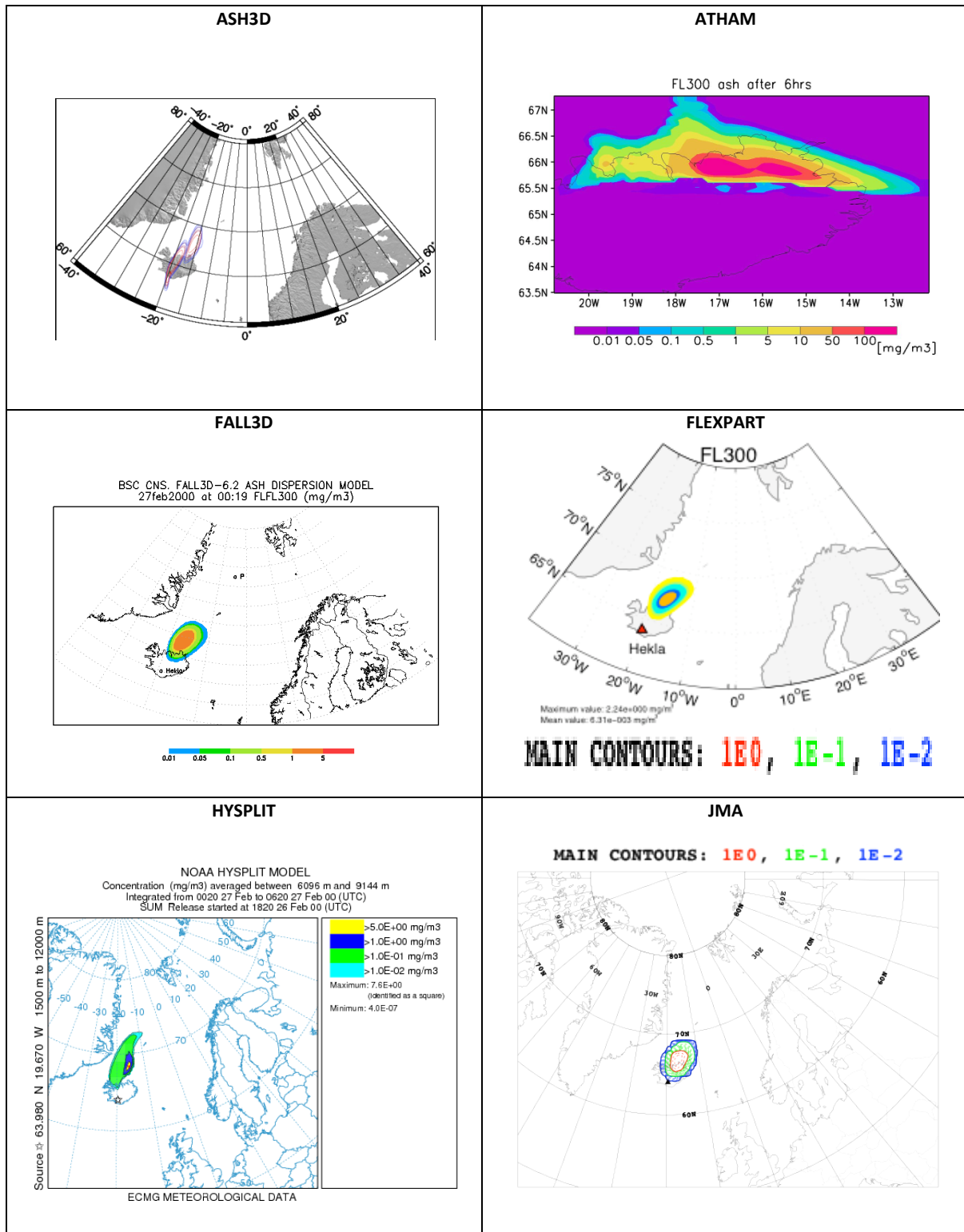


Plate 1.c (cont.)

Concentration contours at FL300 (27 FEB 2000, 00:20UTC, 6h).

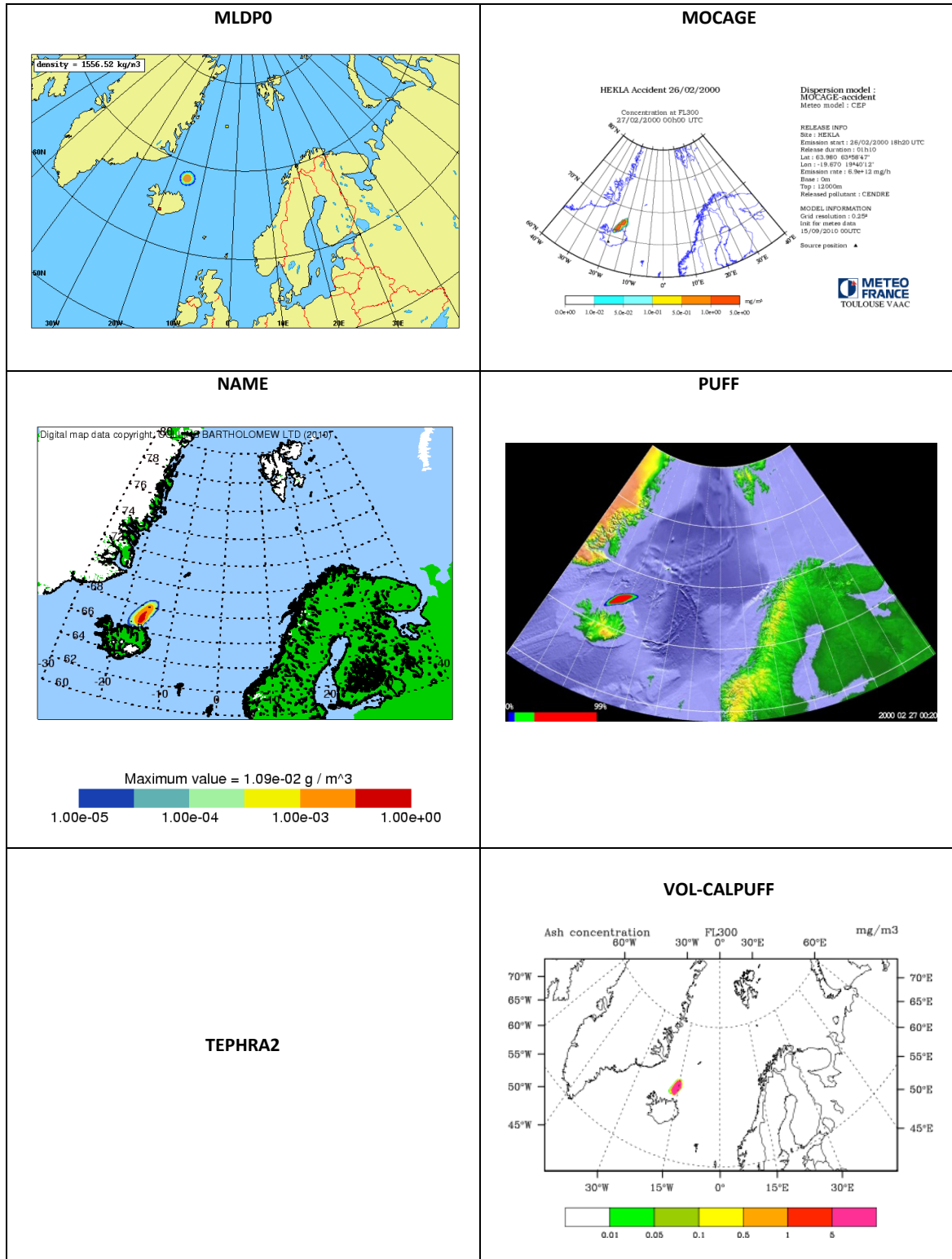


Plate 2.a

Concentration contours at FL100 (27 FEB 2000, 12:20UTC, 18h).

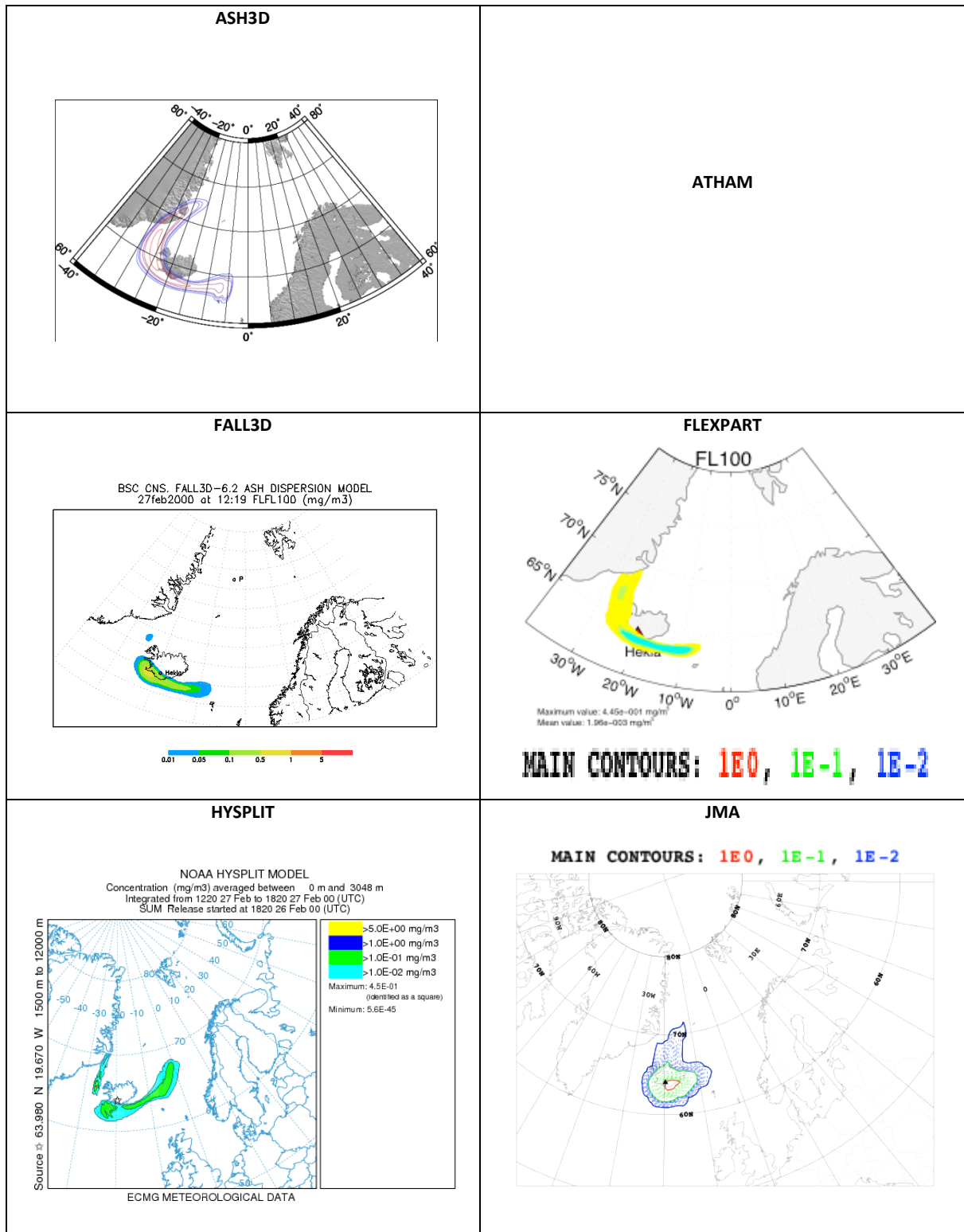




Plate 2.a (cont.)

Concentration contours at FL100 (27 FEB 2000, 12:20UTC, 18h).

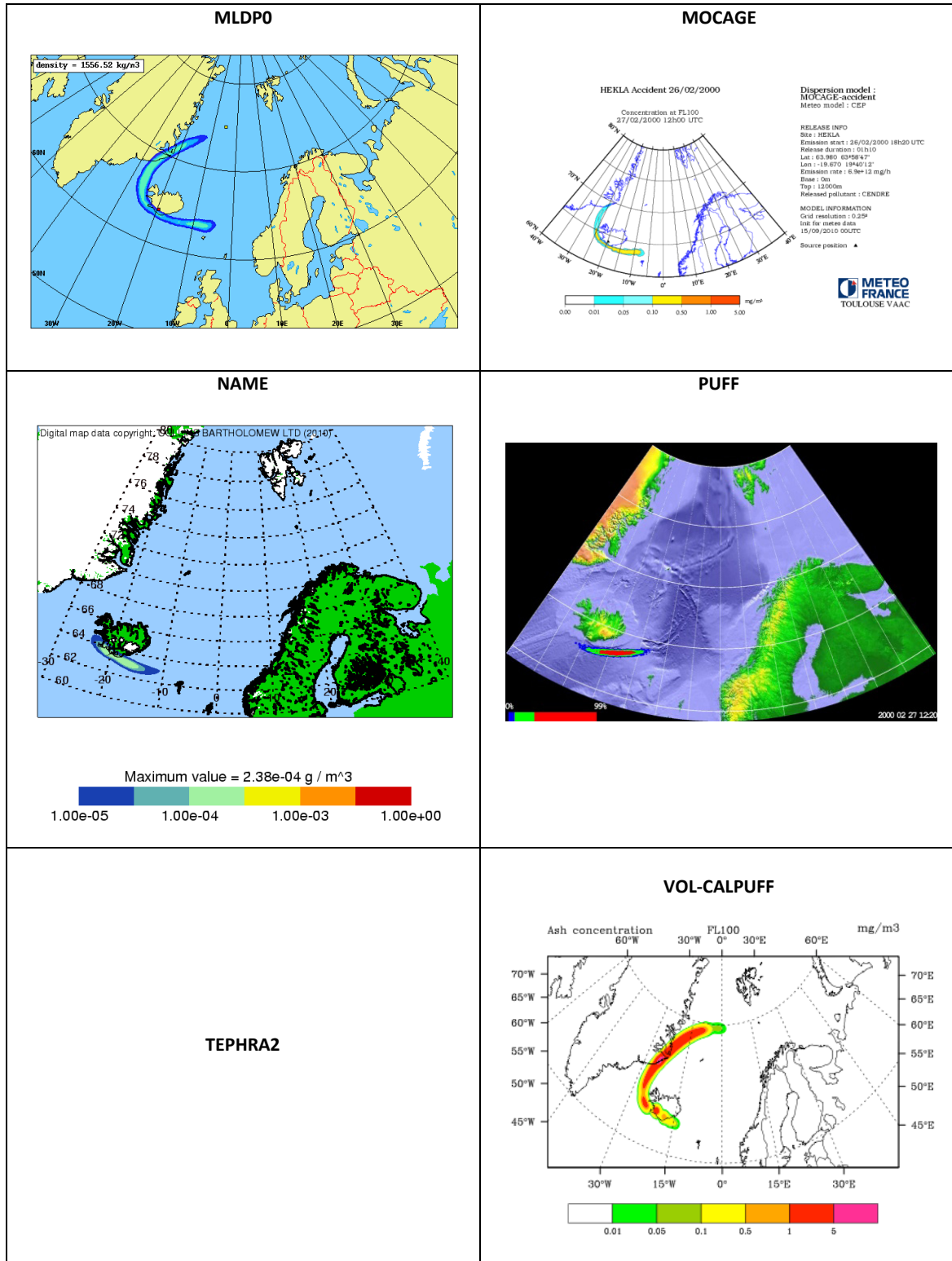


Plate 2.b

Concentration contours at FL200 (27 FEB 2000, 12:20UTC, 18h).

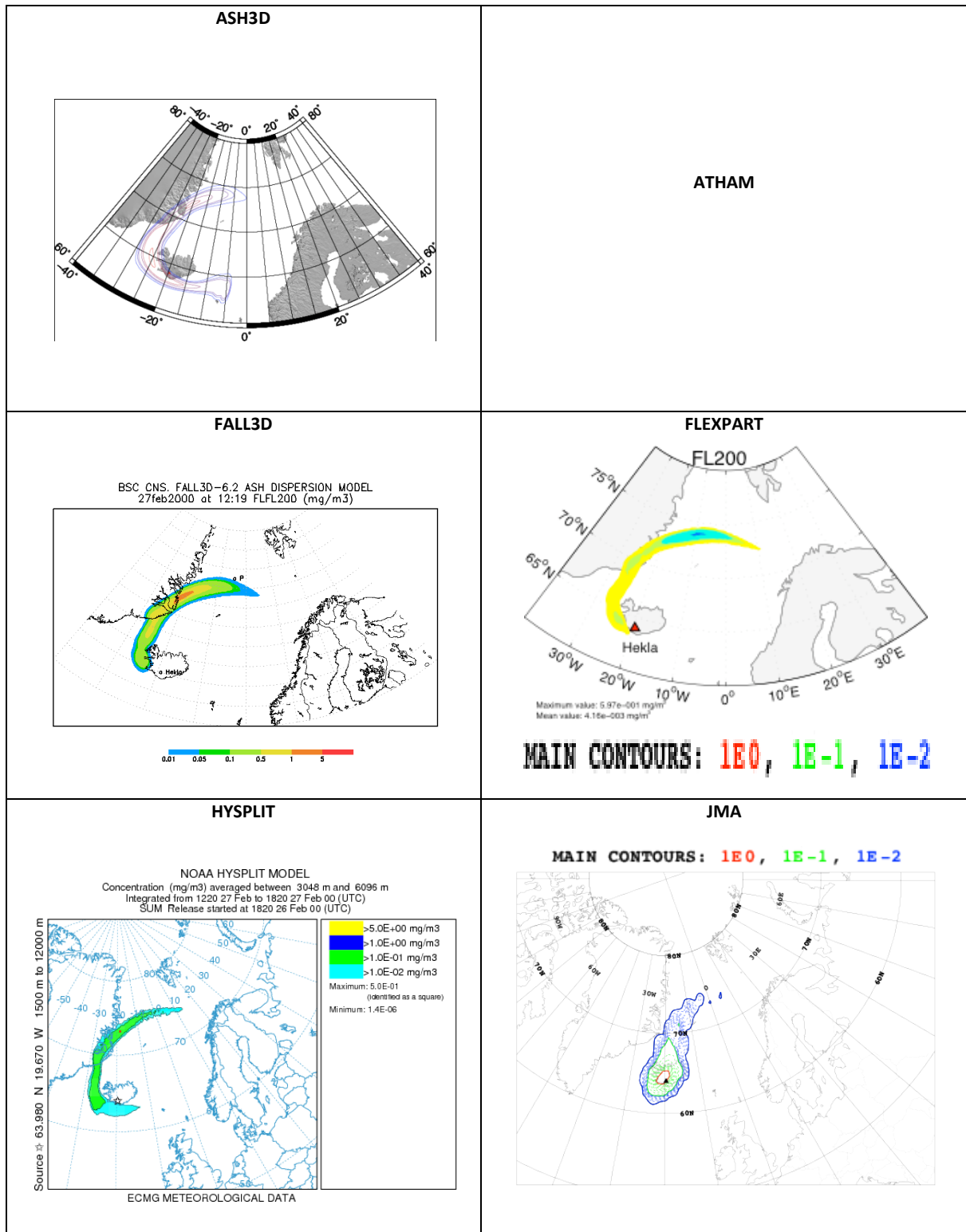




Plate 2.b (cont.)

Concentration contours at FL200 (27 FEB 2000, 12:20UTC, 18h).

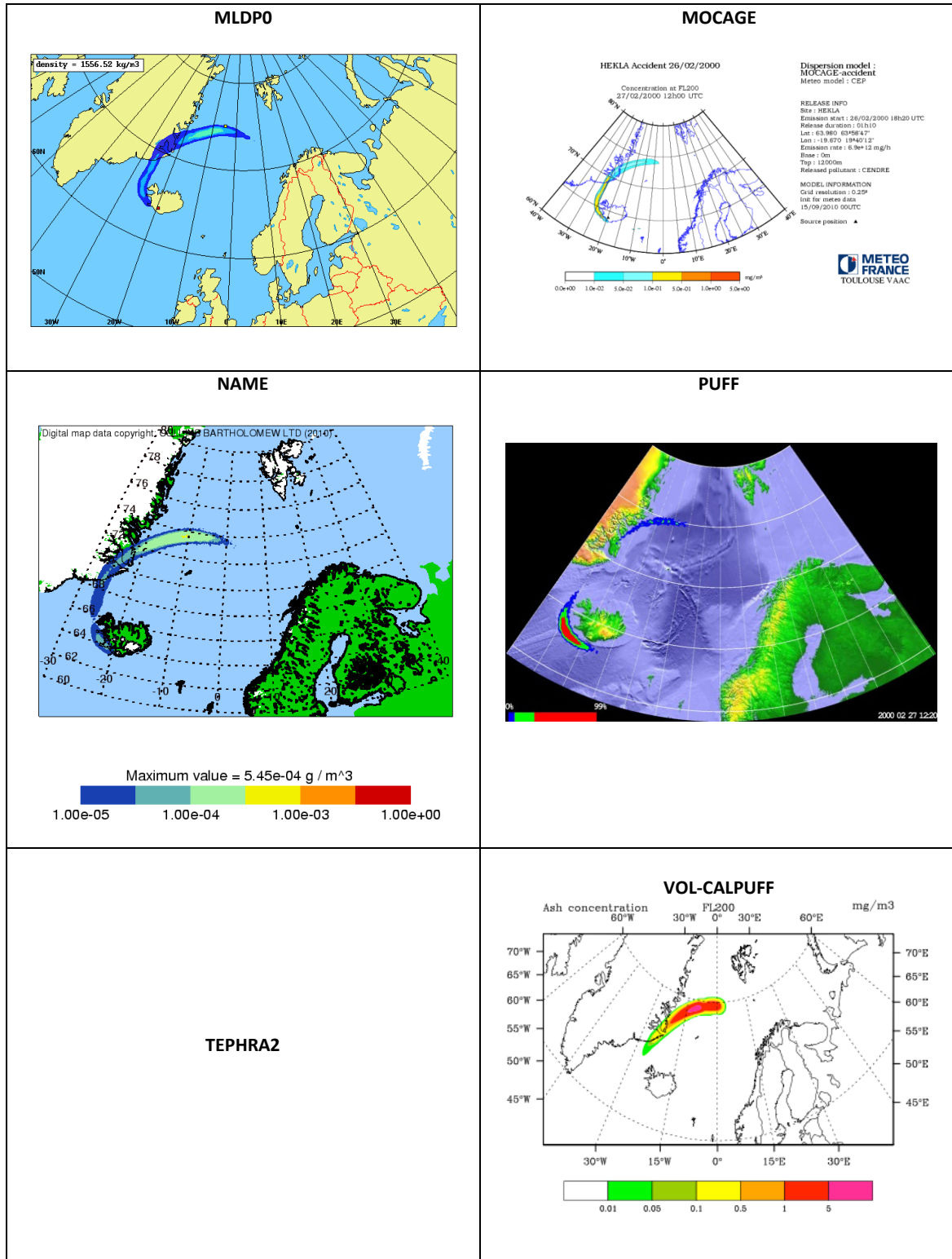




Plate 2.c

Concentration contours at FL300 (27 FEB 2000, 12:20UTC, 18h).

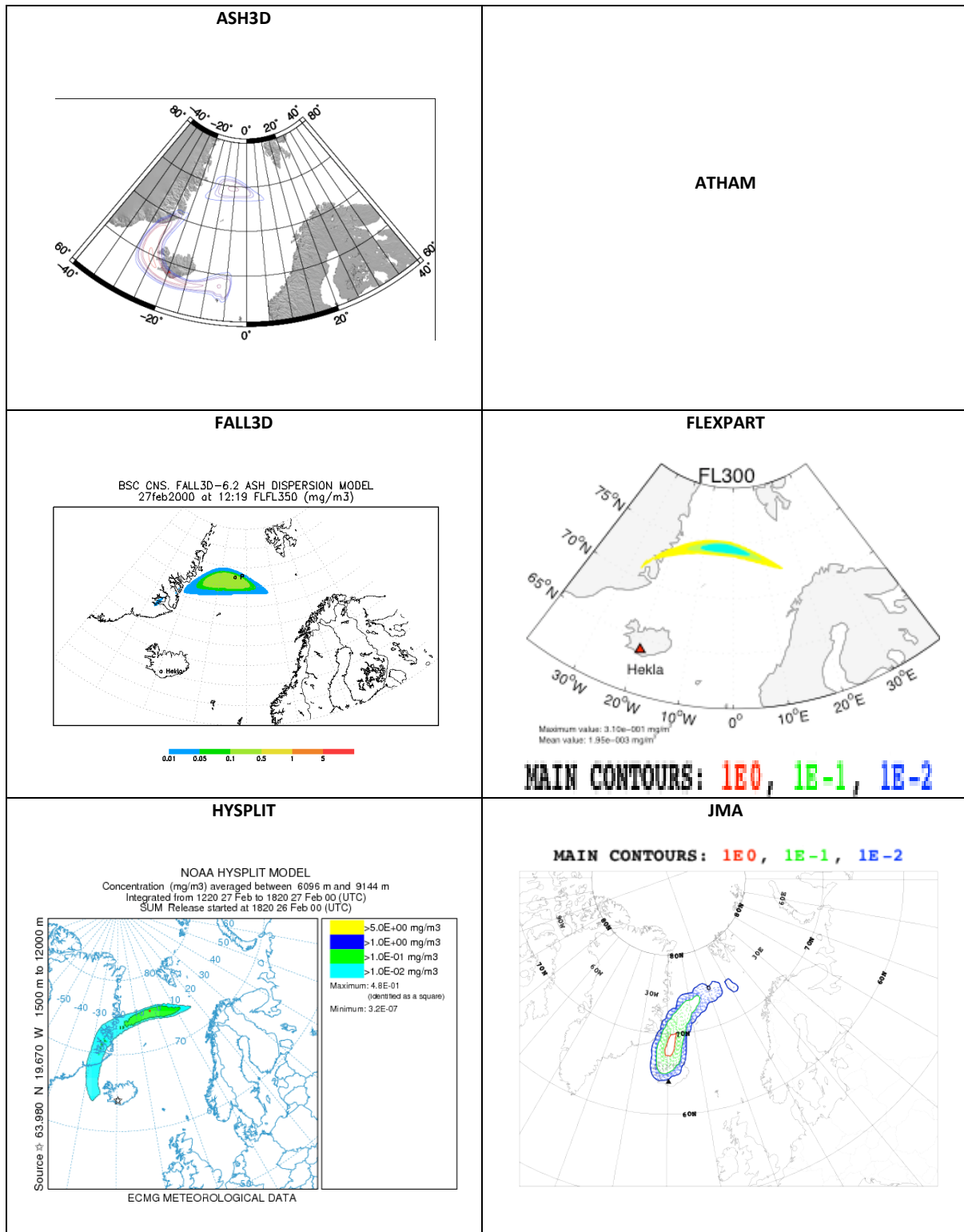


Plate 2.c (cont.)

Concentration contours at FL300 (27 FEB 2000, 12:20UTC, 18h).

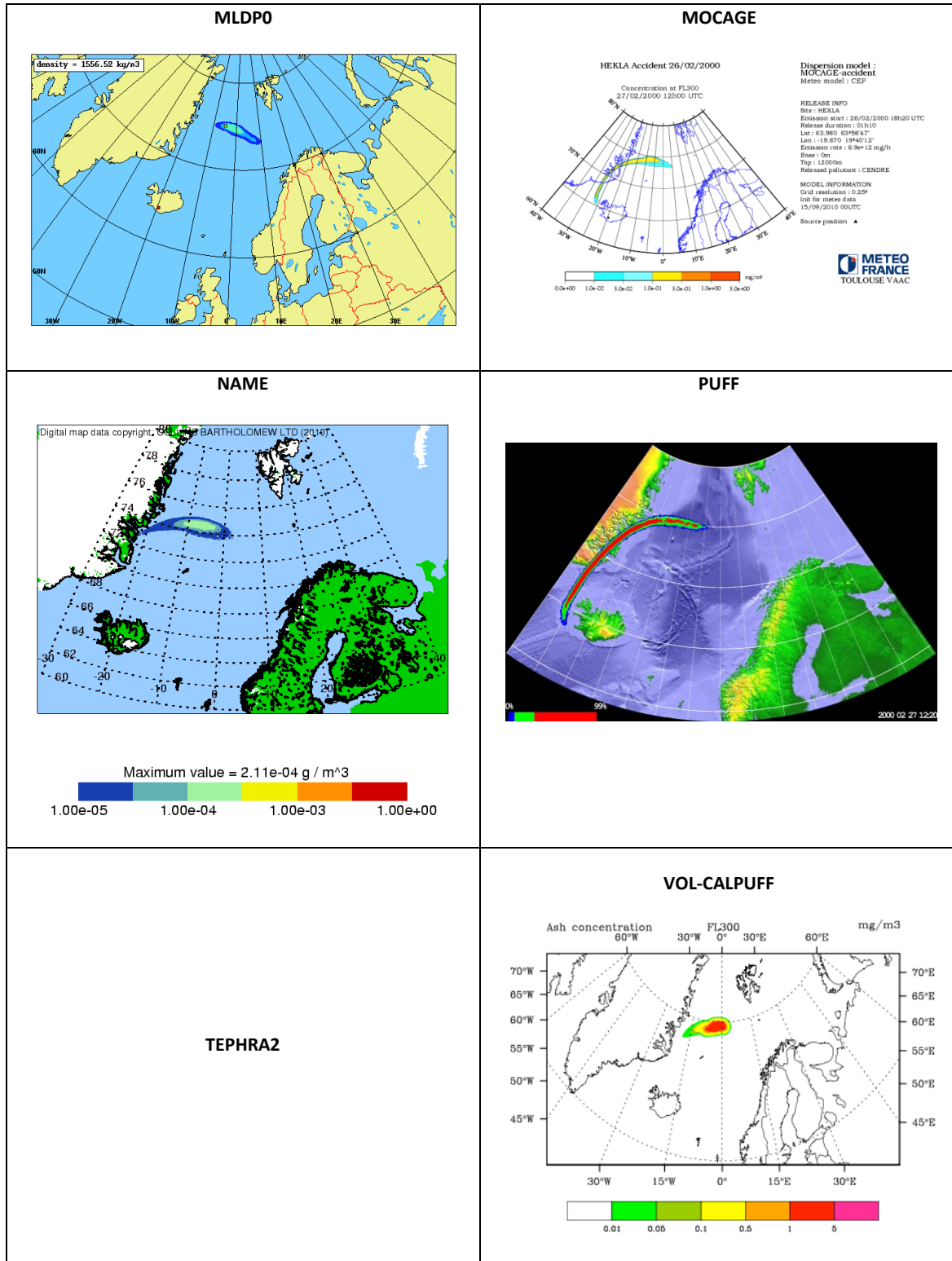




Plate 3.a

Concentration contours at FL100 (28 FEB 2000, 00:20UTC, 30h).

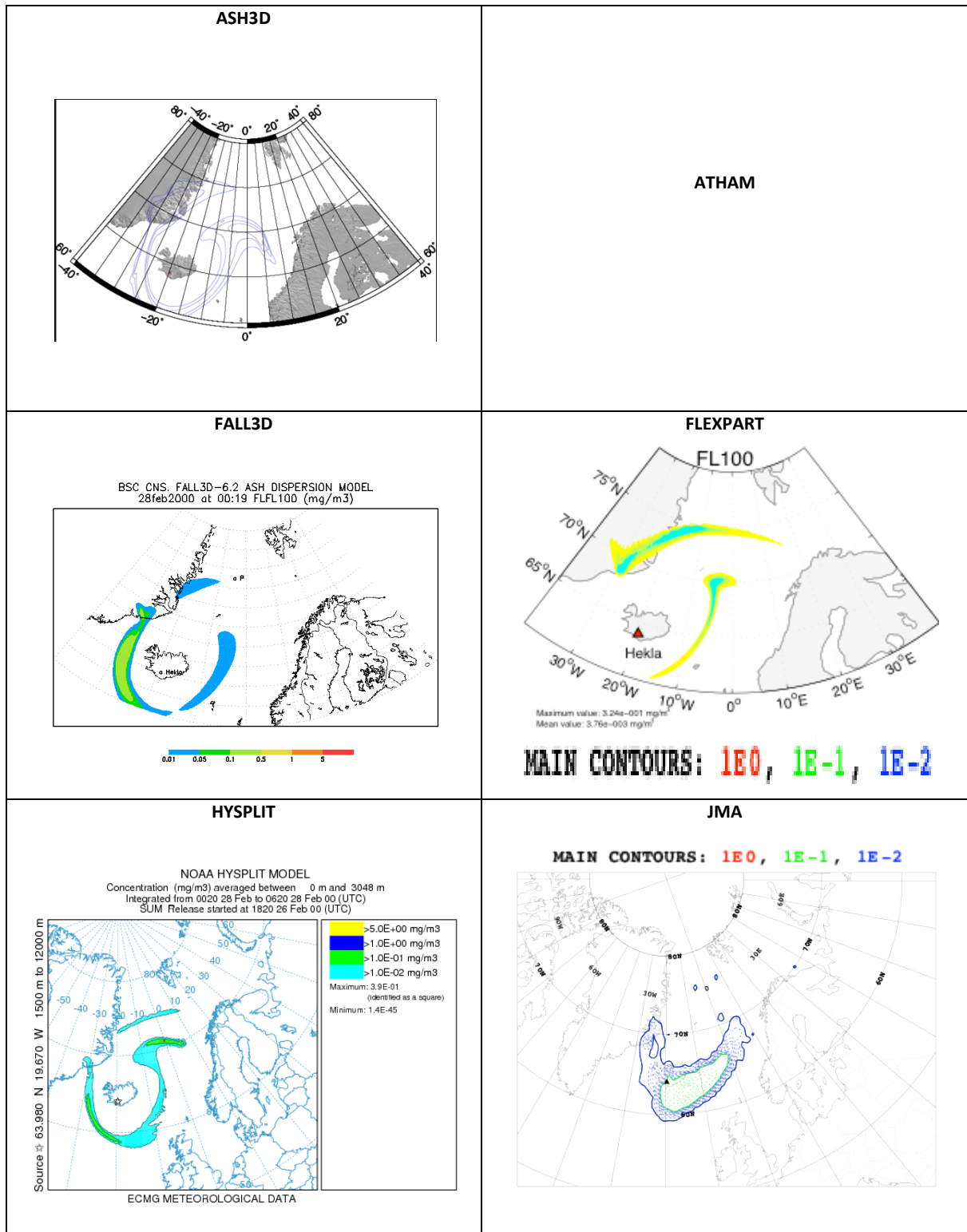




Plate 3.a (cont.)

Concentration contours at FL100 (28 FEB 2000, 00:20UTC, 30h).

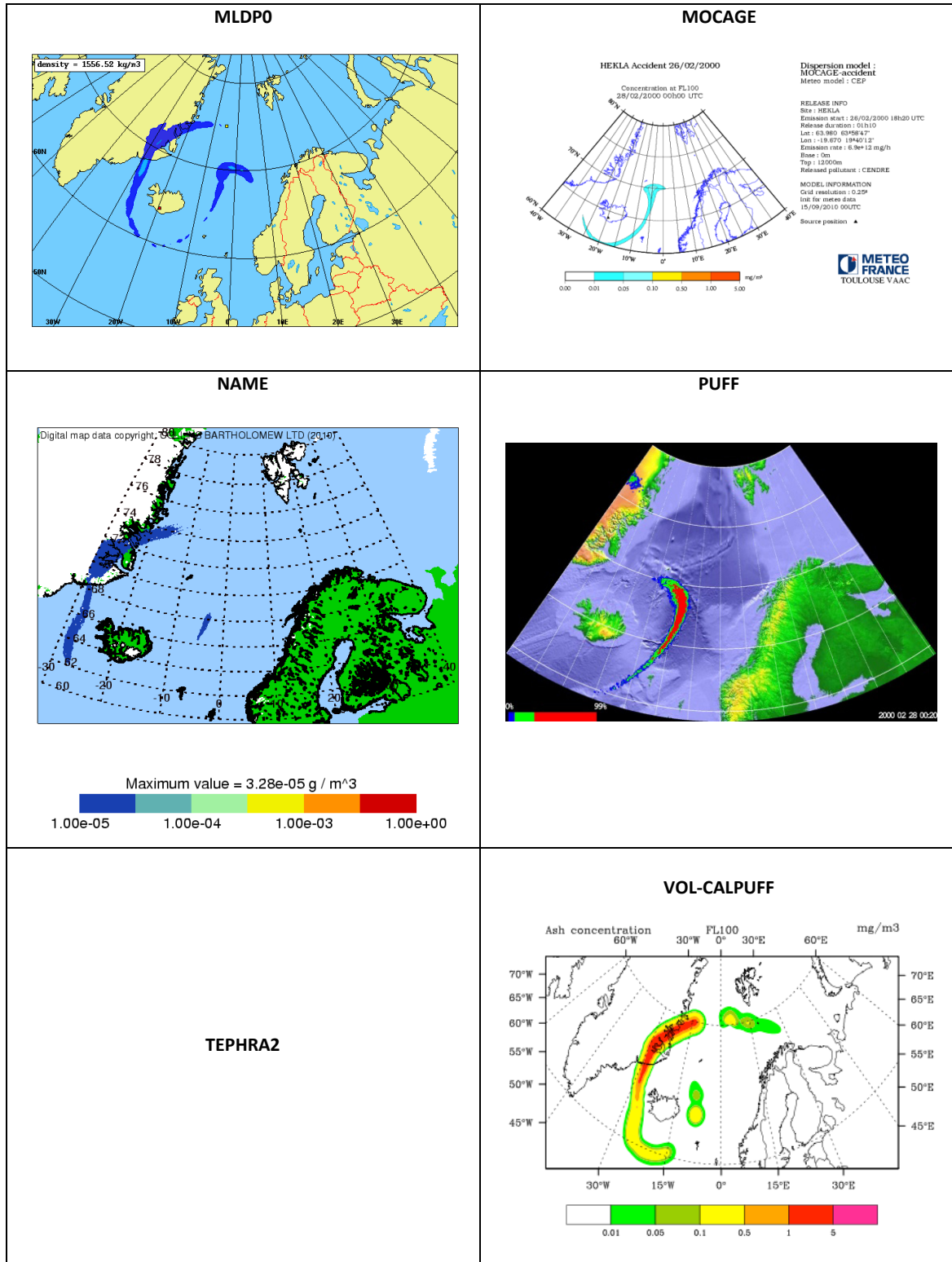




Plate 3.b

Concentration contours at FL200 (28 FEB 2000, 00:20UTC, 30h).

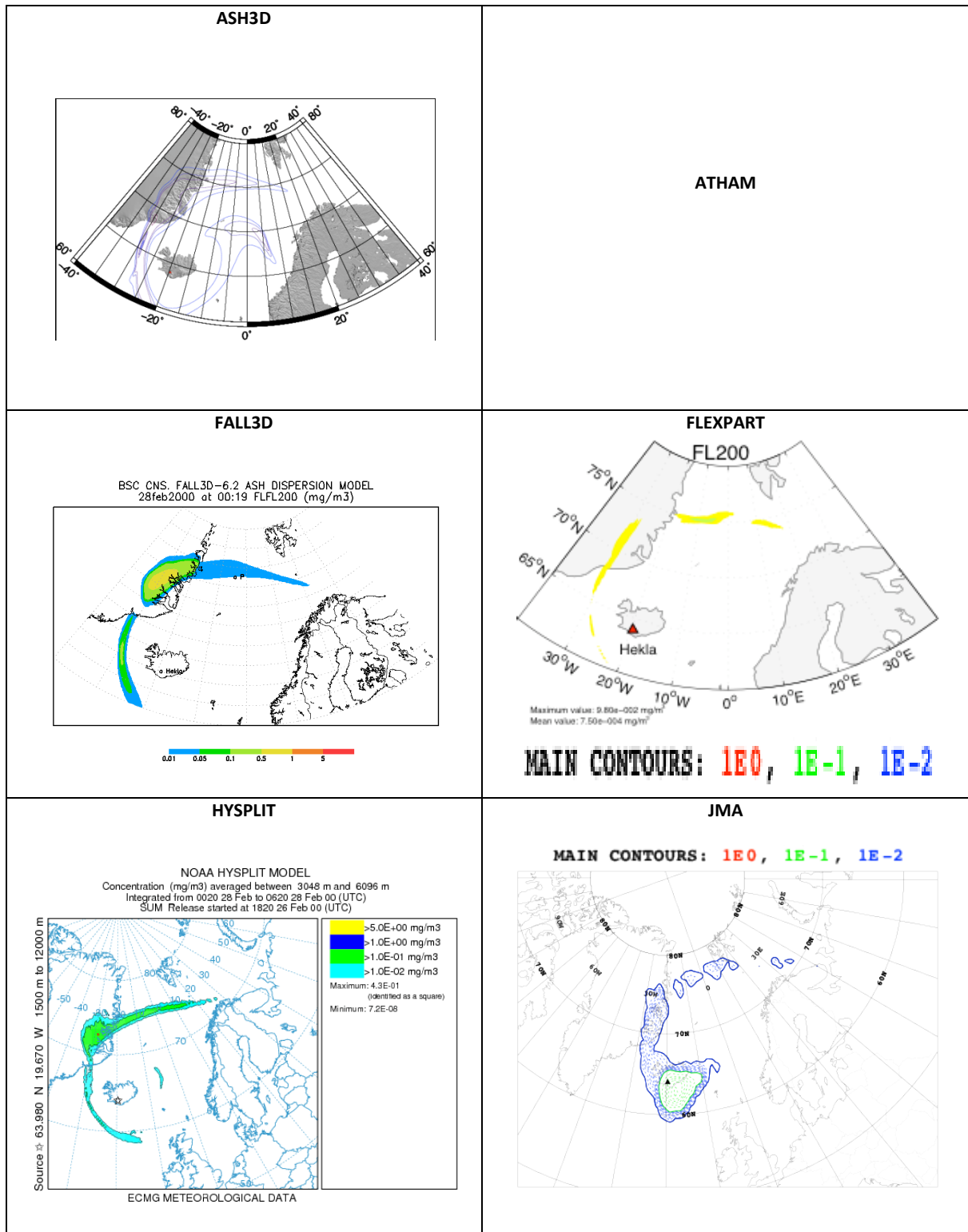


Plate 3.b (cont.)

Concentration contours at FL200 (28 FEB 2000, 00:20UTC, 30h).

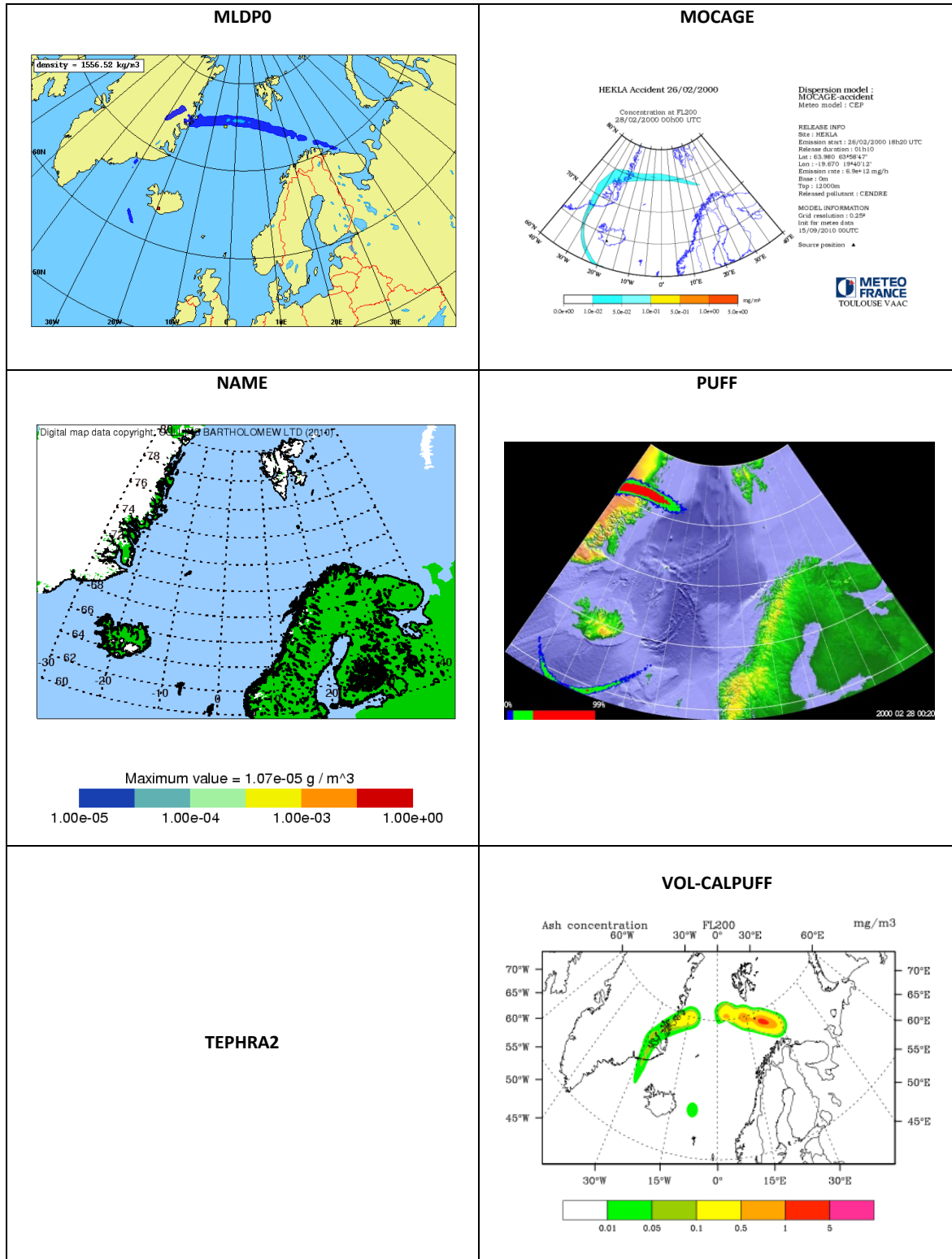


Plate 3.c

Concentration contours at FL300 (28 FEB 2000, 00:20UTC, 30h).

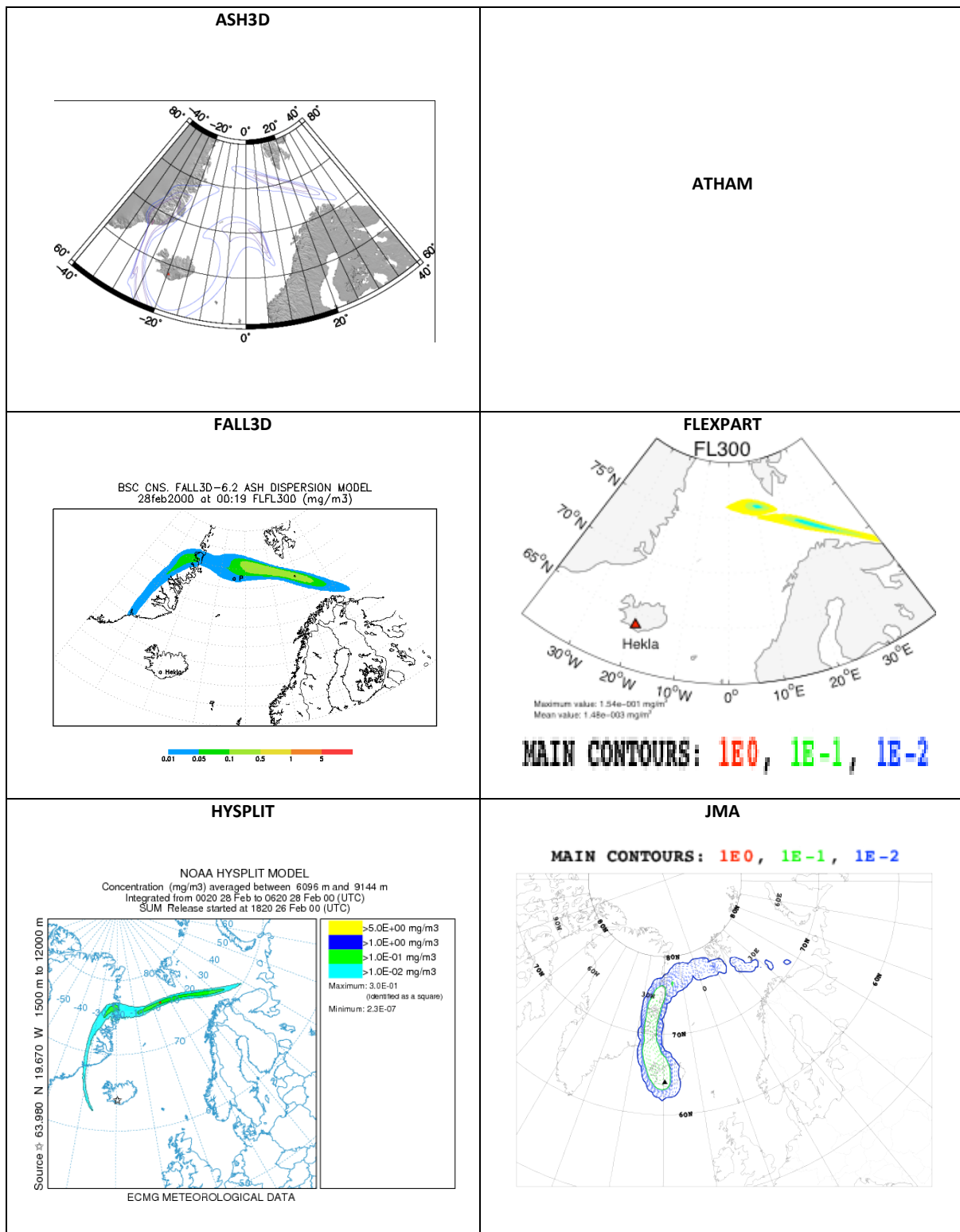


Plate 3.c (cont.)

Concentration contours at FL300 (28 FEB 2000, 00:20UTC, 30h).

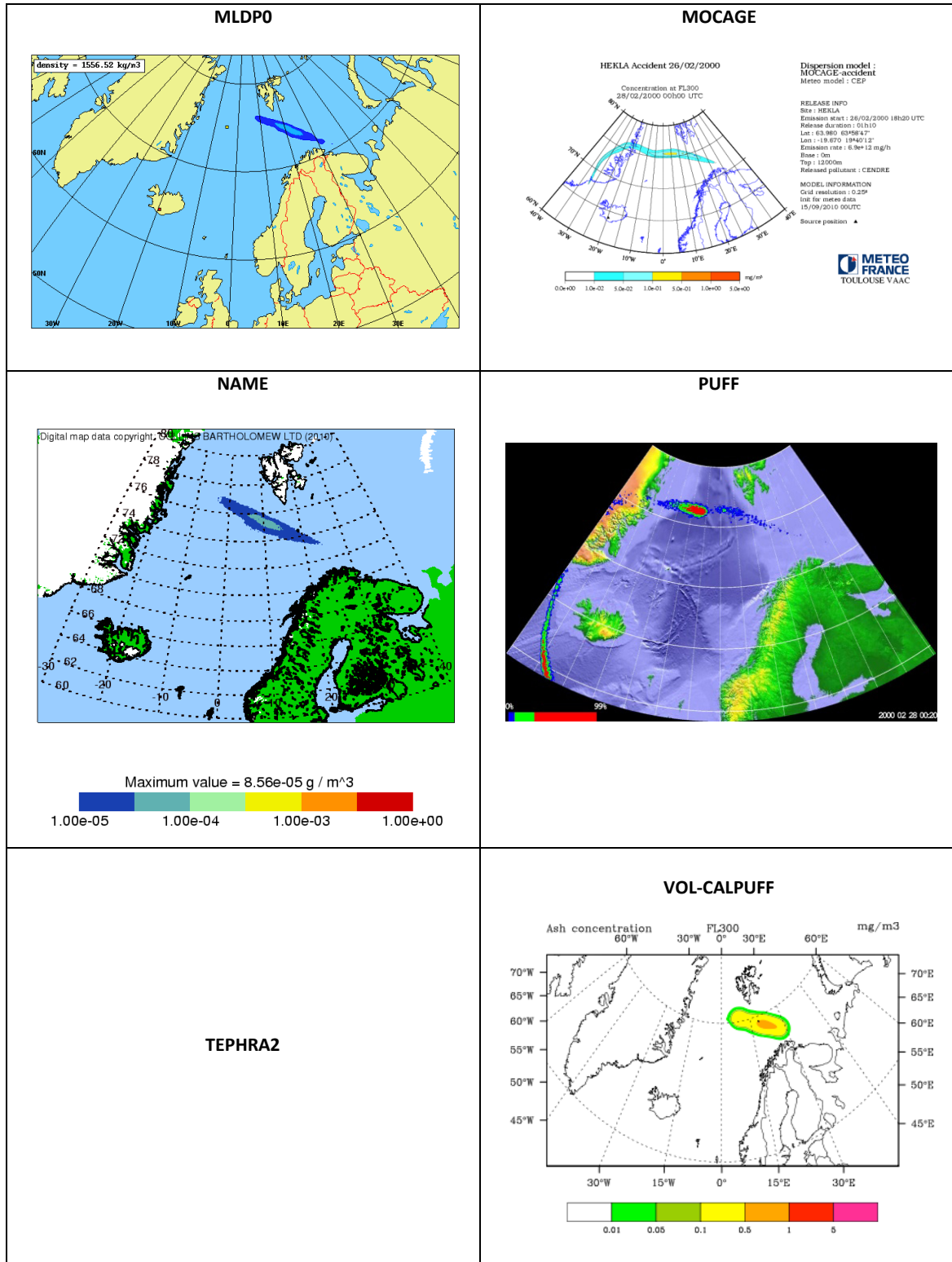




Plate 4.a

Concentration contours at FL100 (28 FEB 2000, 12:20UTC, 42h).

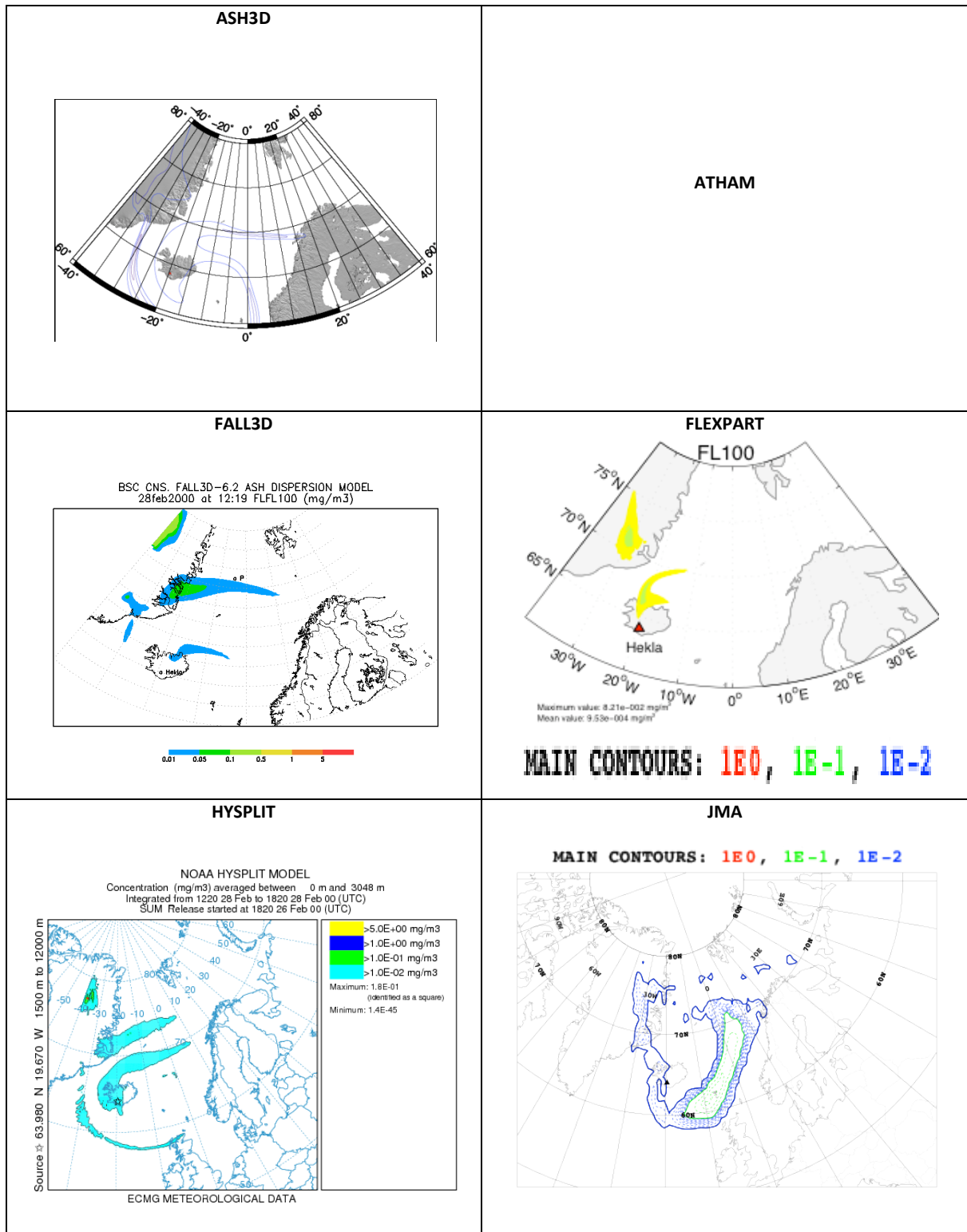


Plate 4.a (cont.)

Concentration contours at FL100 (28 FEB 2000, 12:20UTC, 42h).

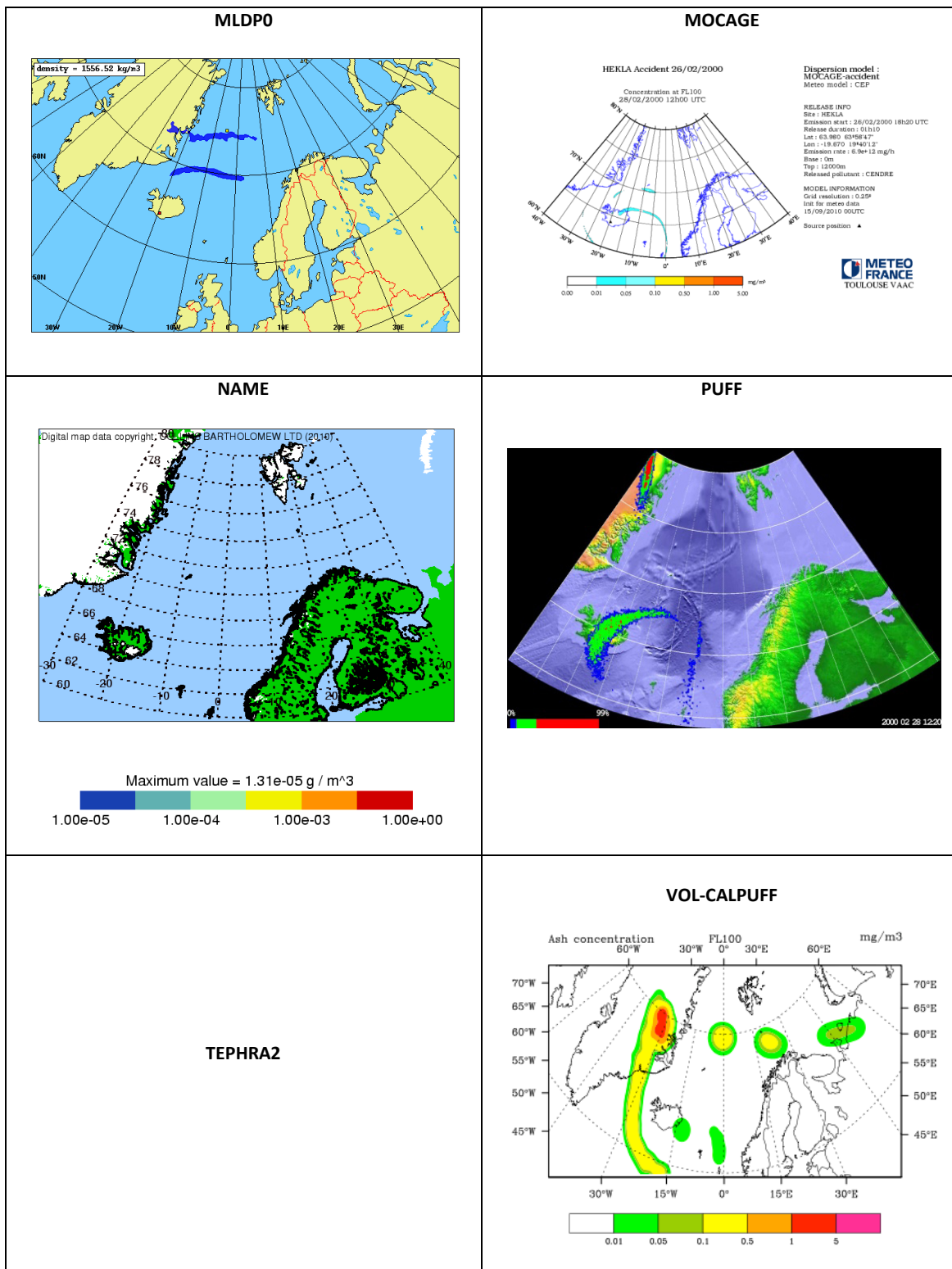


Plate 4.b

Concentration contours at FL200 (28 FEB 2000, 12:20UTC, 42h).

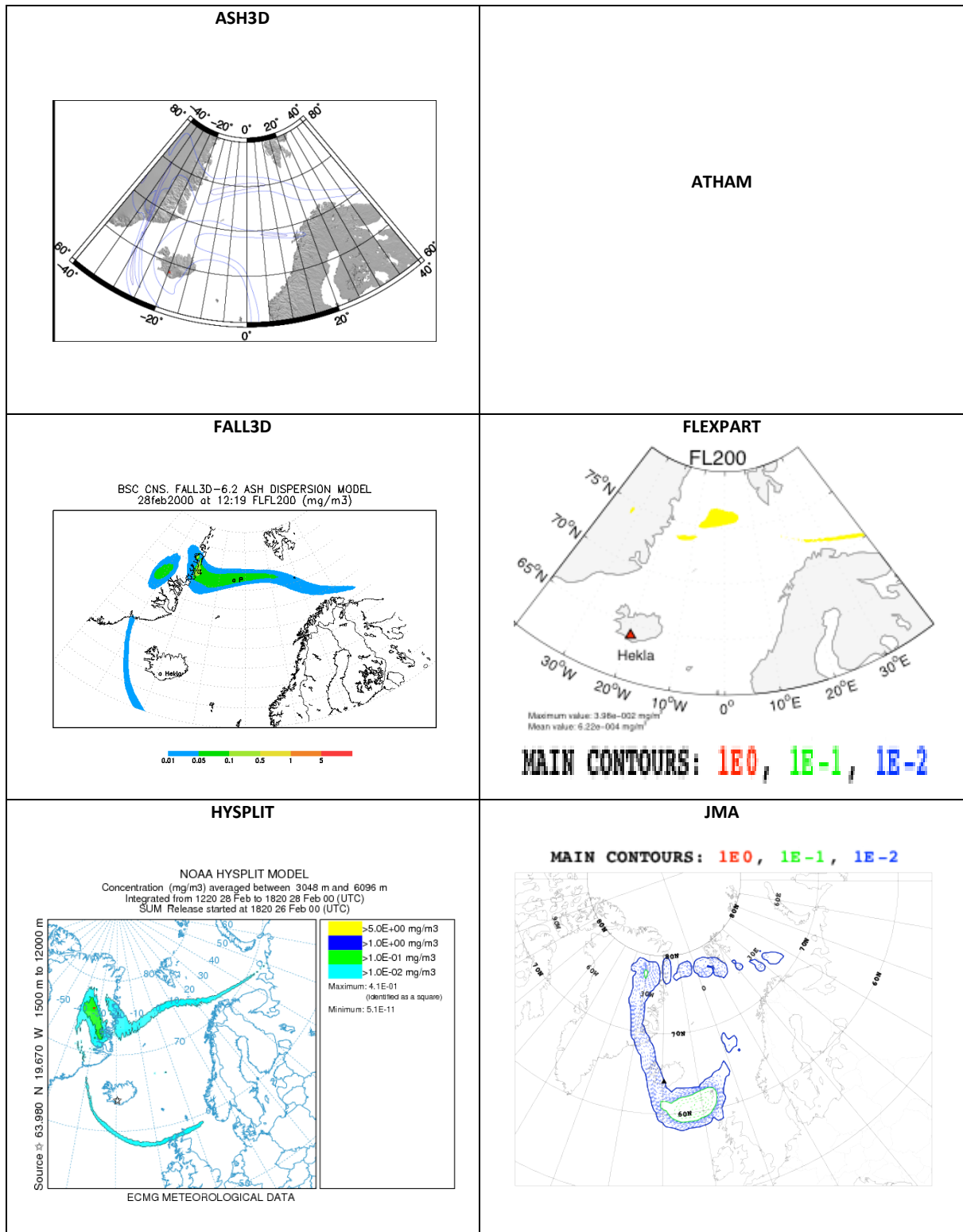


Plate 4.b (cont.)

Concentration contours at FL200 (28 FEB 2000, 12:20UTC, 42h).

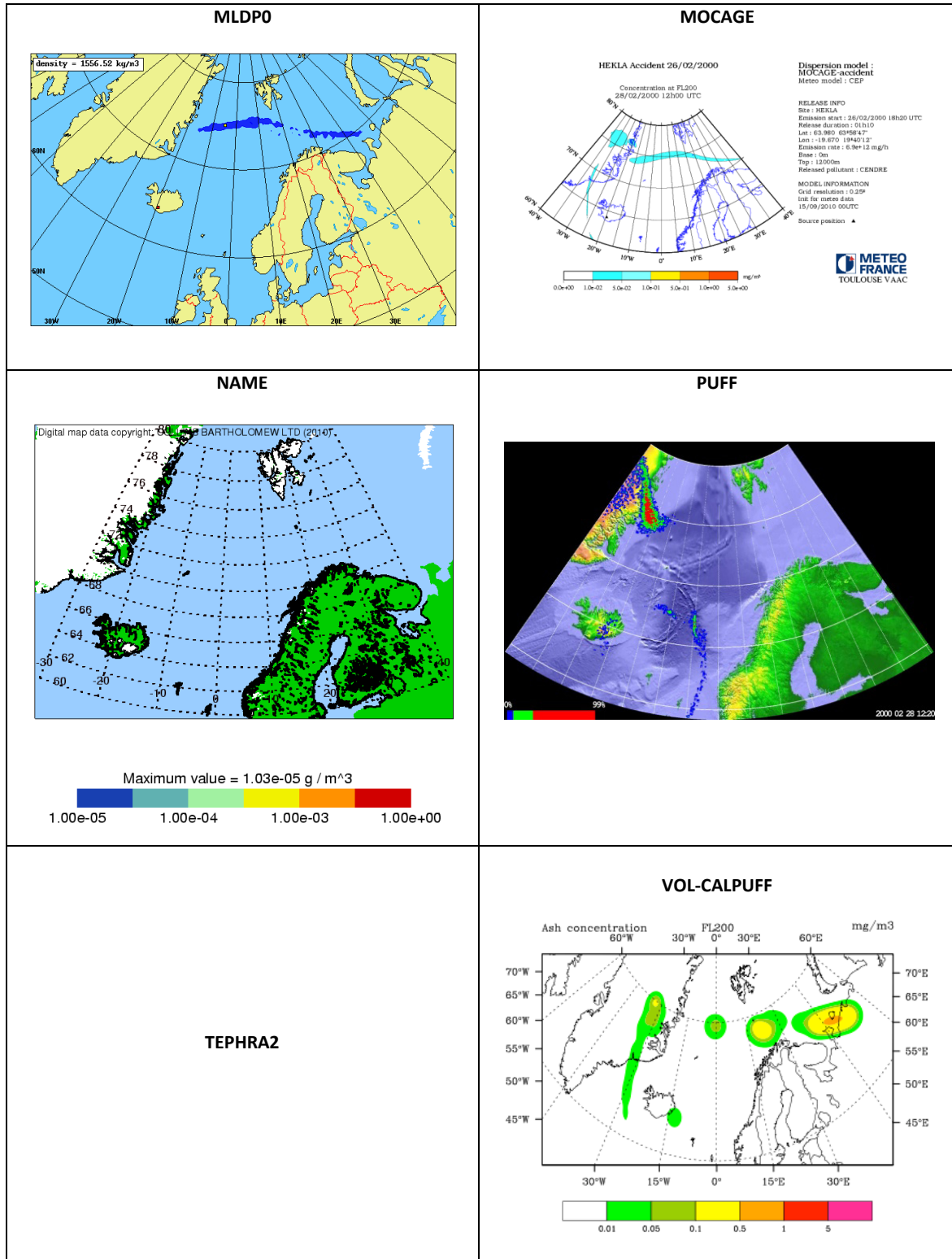




Plate 4.c

Concentration contours at FL300 (28 FEB 2000, 12:20UTC, 42h).

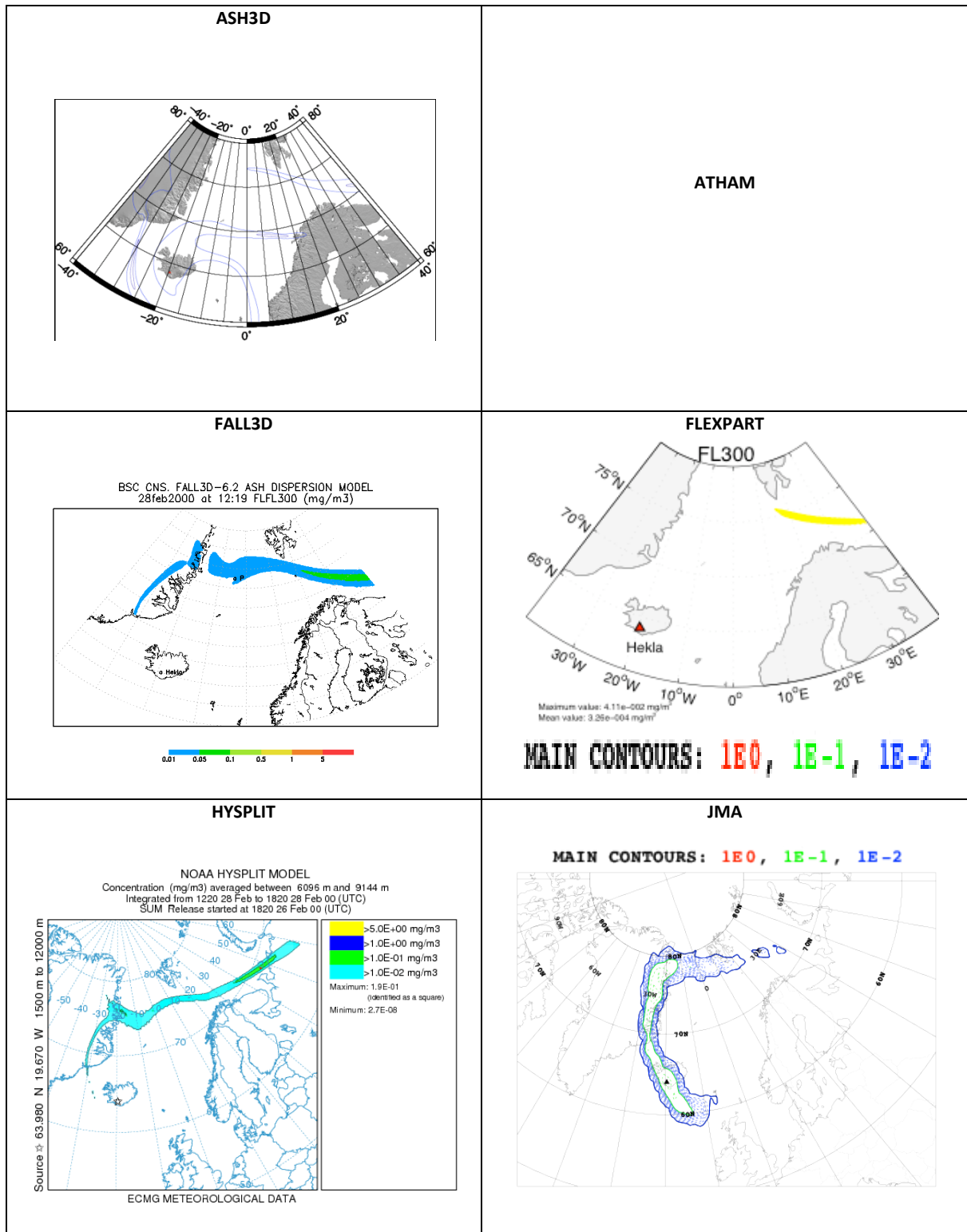


Plate 4.c (cont.)

Concentration contours at FL300 (28 FEB 2000, 12:20UTC, 42h).

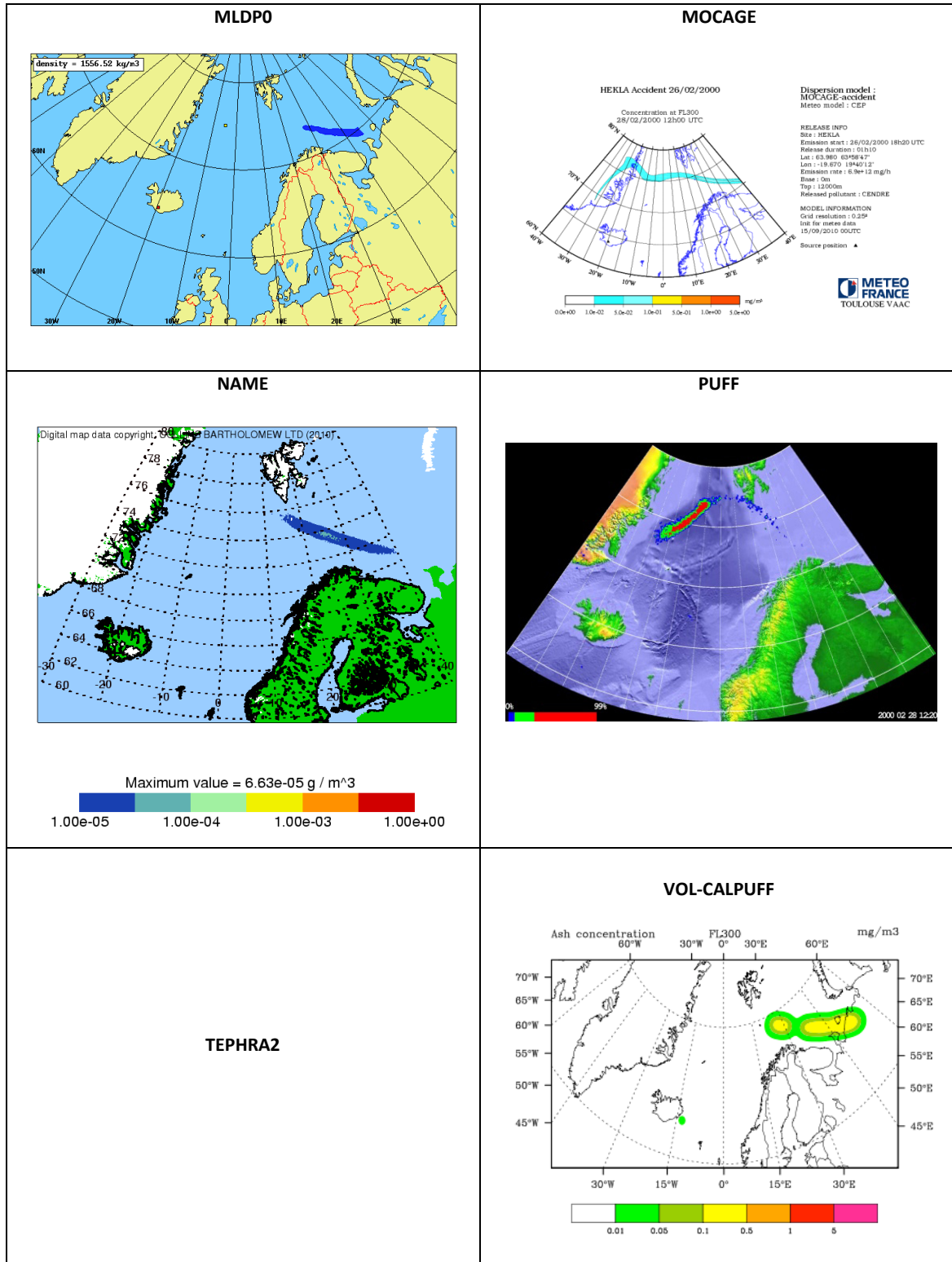




Plate 5.a

Concentration contours at FL100 (29 FEB 2000, 00:20UTC, 54h).

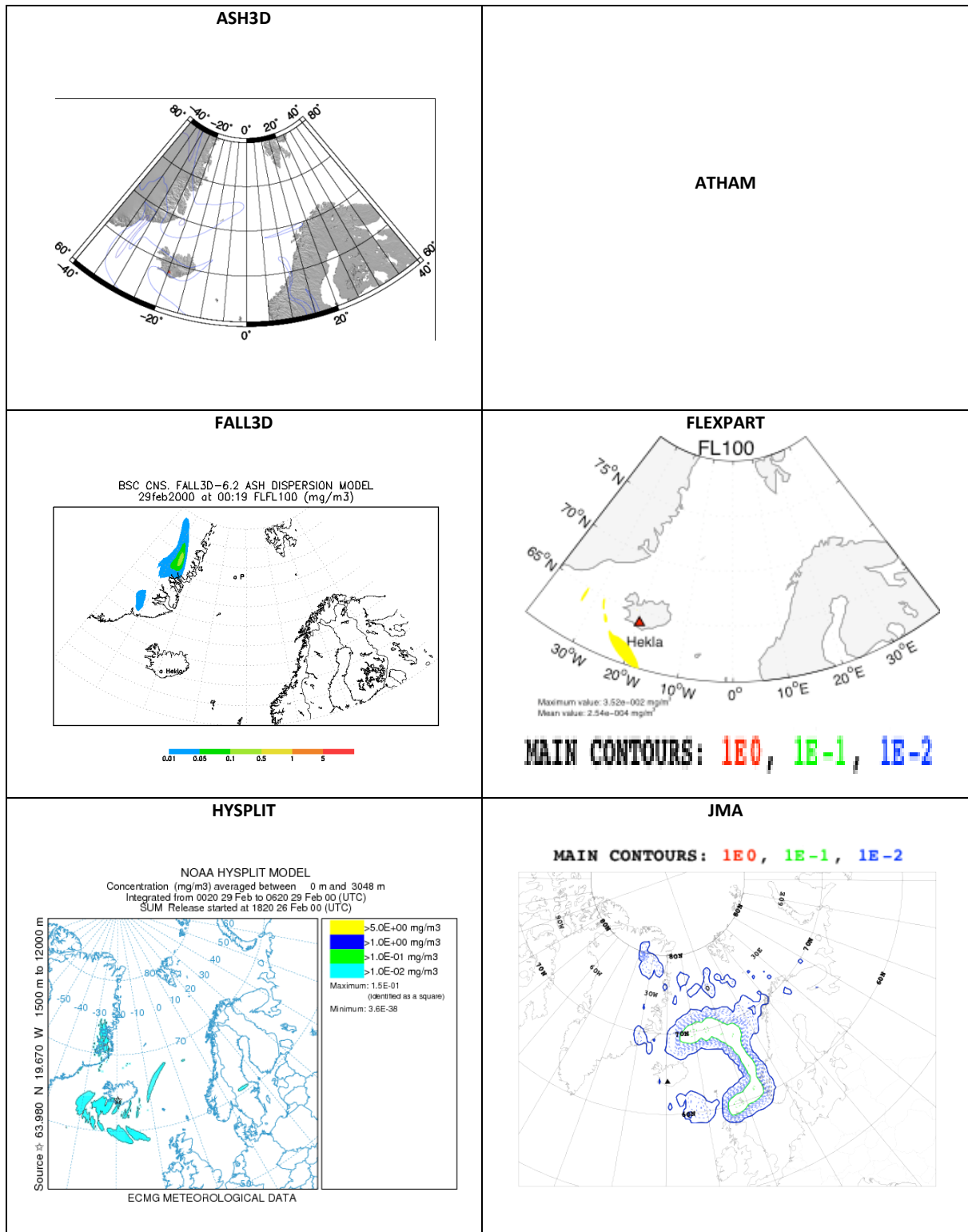


Plate 5.a (cont.)

Concentration contours at FL100 (29 FEB 2000, 00:20UTC, 54h).

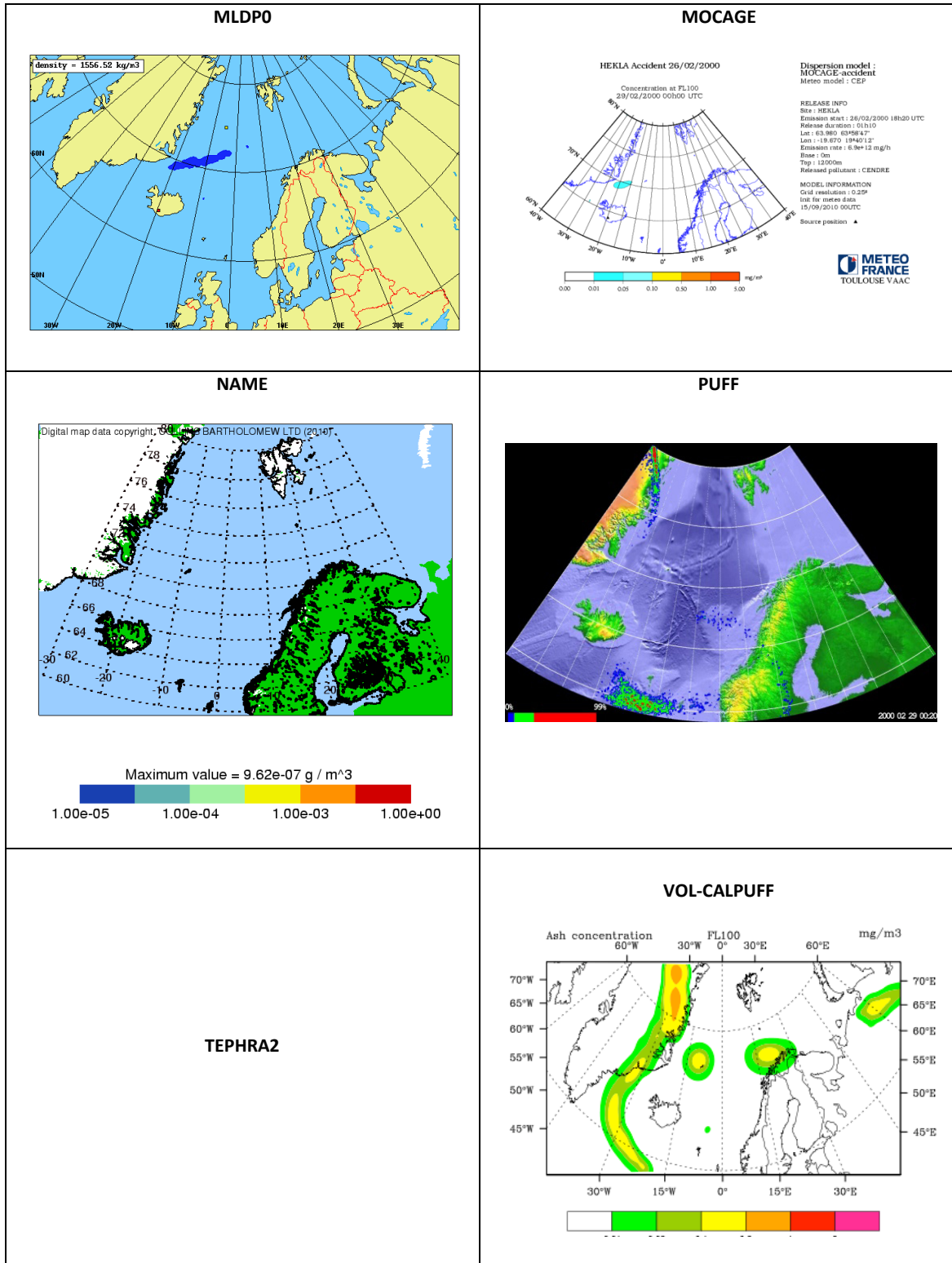




Plate 5.b

Concentration contours at FL200 (29 FEB 2000, 00:20UTC, 54h).

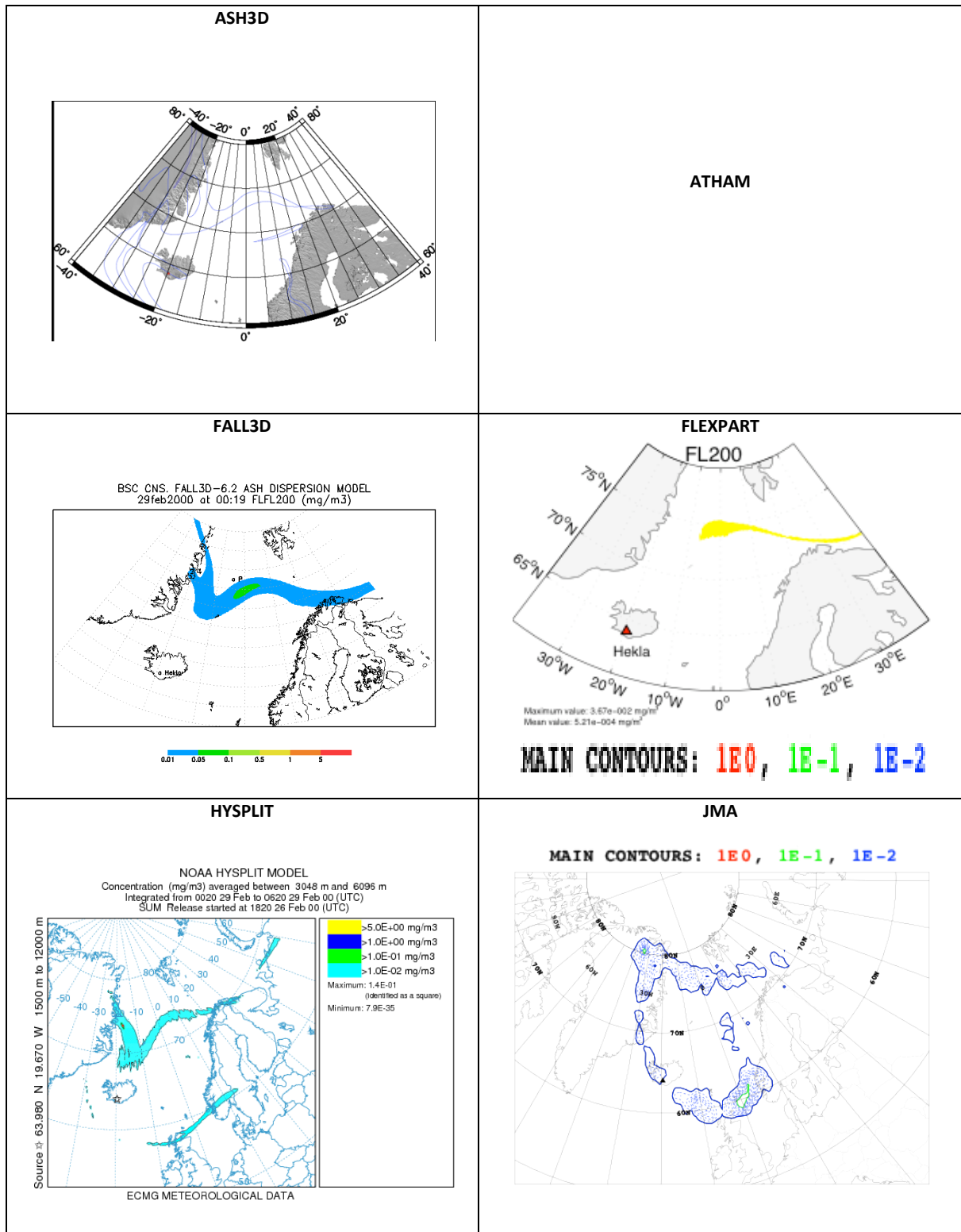


Plate 5.b (cont.)

Concentration contours at FL200 (29 FEB 2000, 00:20UTC, 54h).

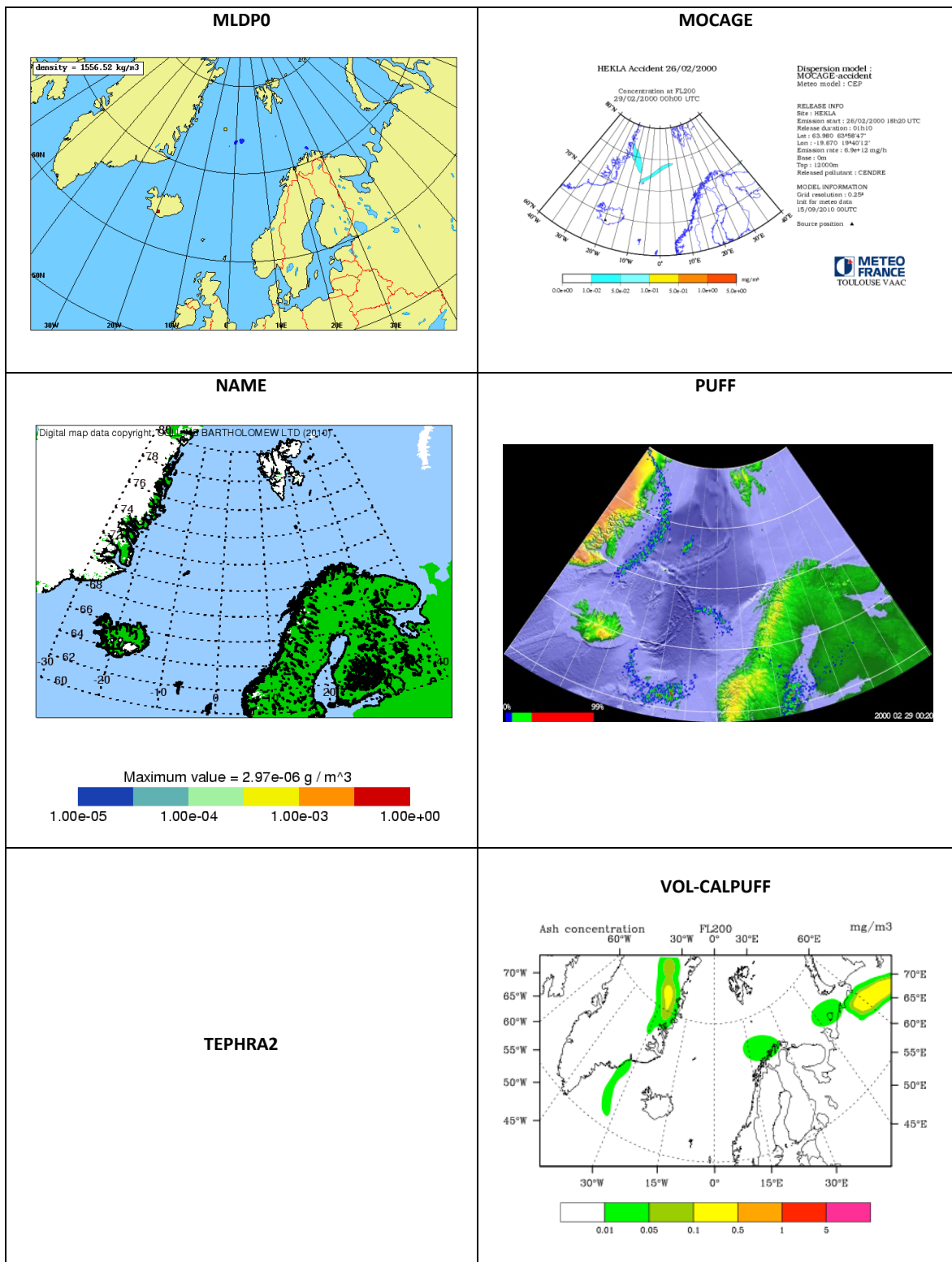




Plate 5.c

Concentration contours at FL300 (29 FEB 2000, 00:20UTC, 54h).

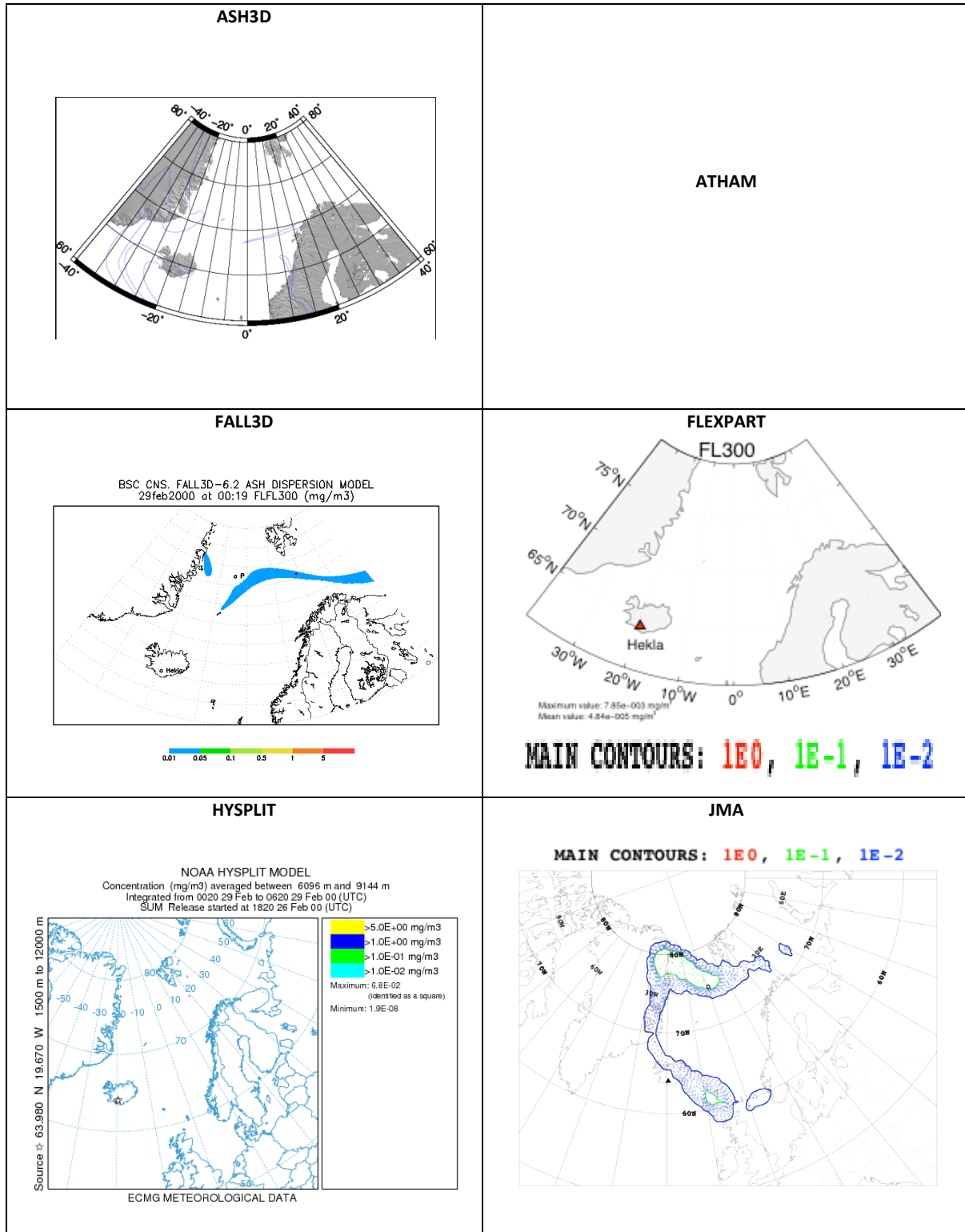


Plate 5.c (cont.)

Concentration contours at FL300 (29 FEB 2000, 00:20UTC, 54h).

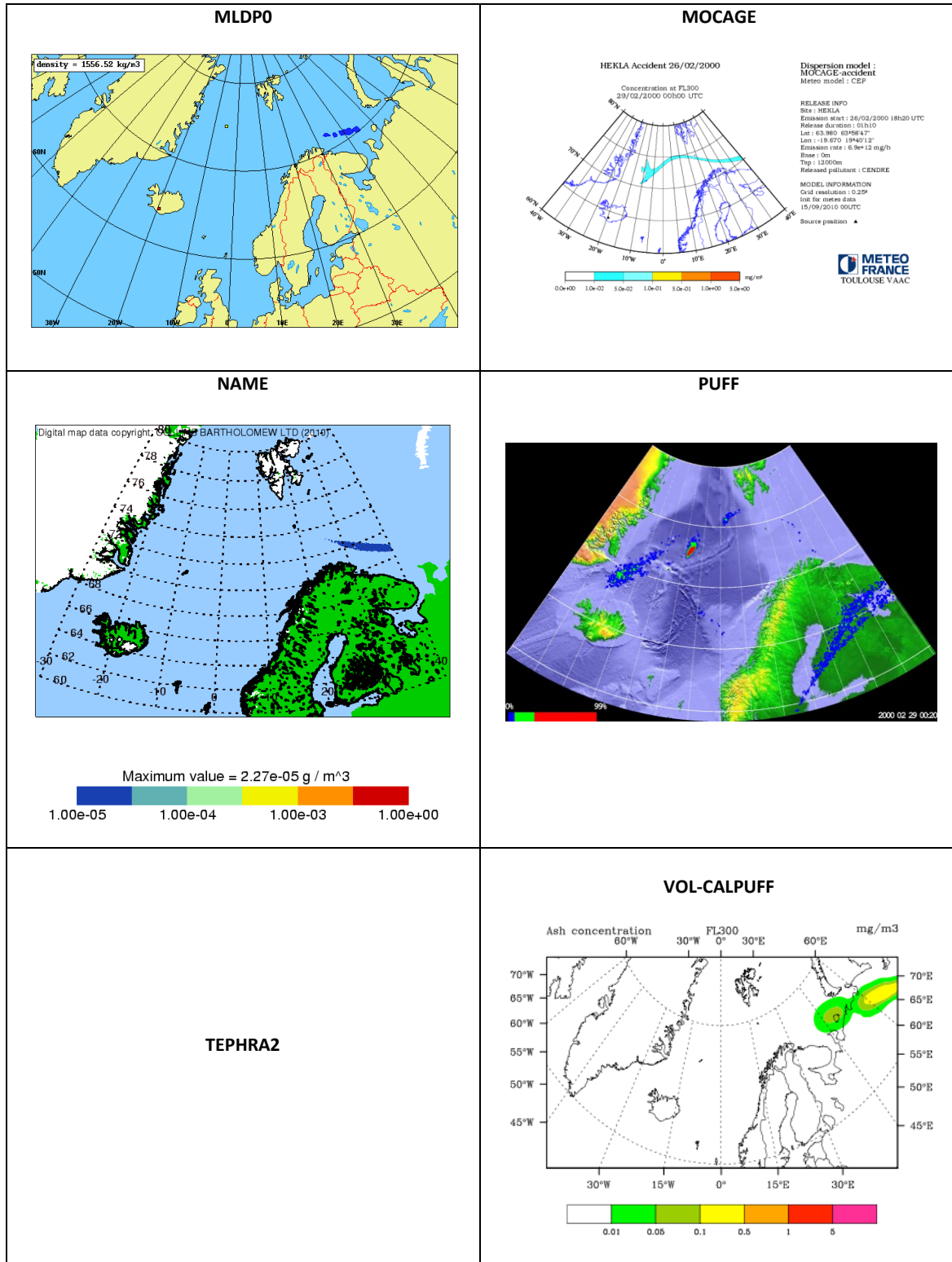




Plate 6.a

Concentration contours at FL100 (29 FEB 2000, 12:20UTC, 66h).

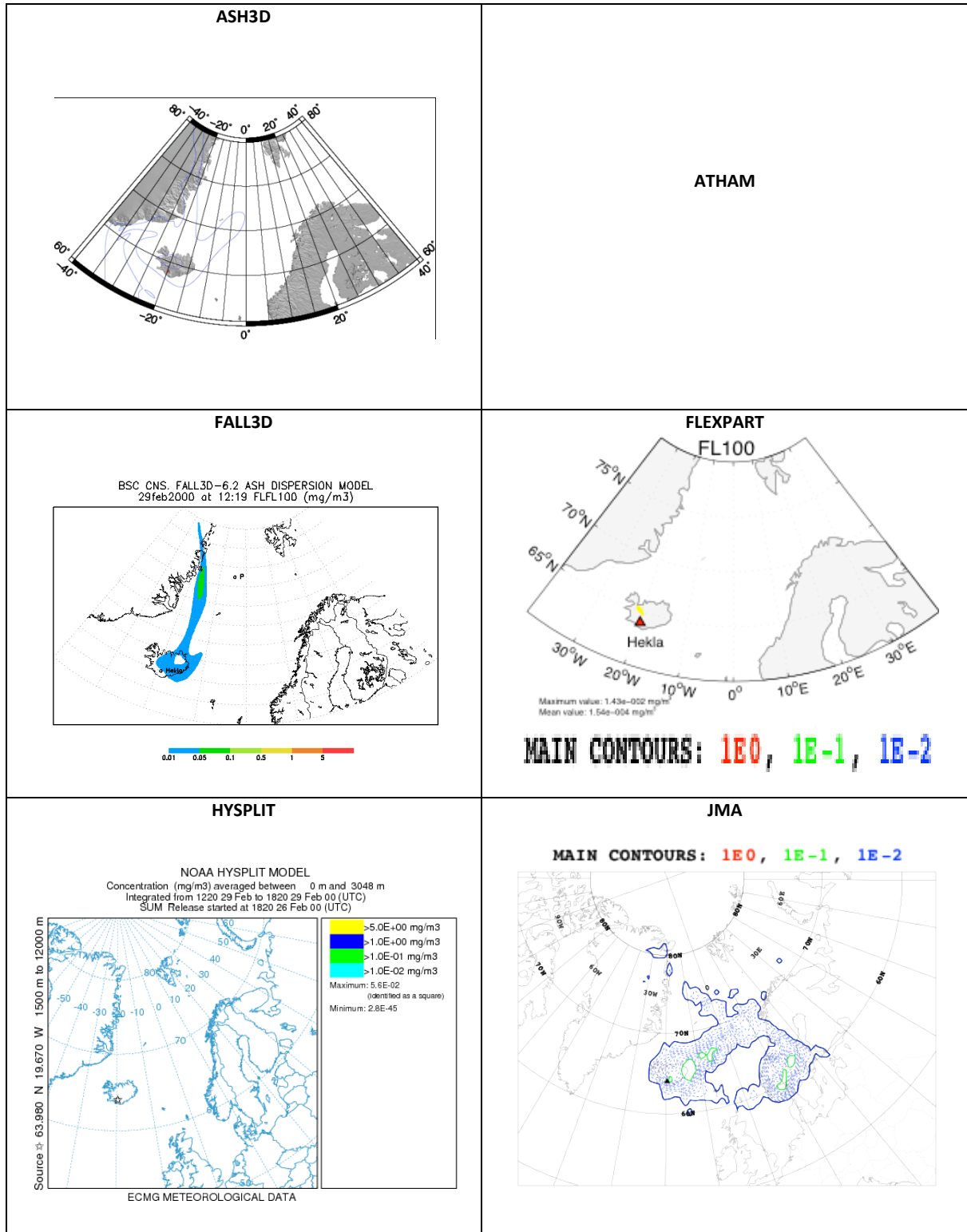




Plate 6.a (cont.)

Concentration contours at FL100 (29 FEB 2000, 12:20UTC, 66h).

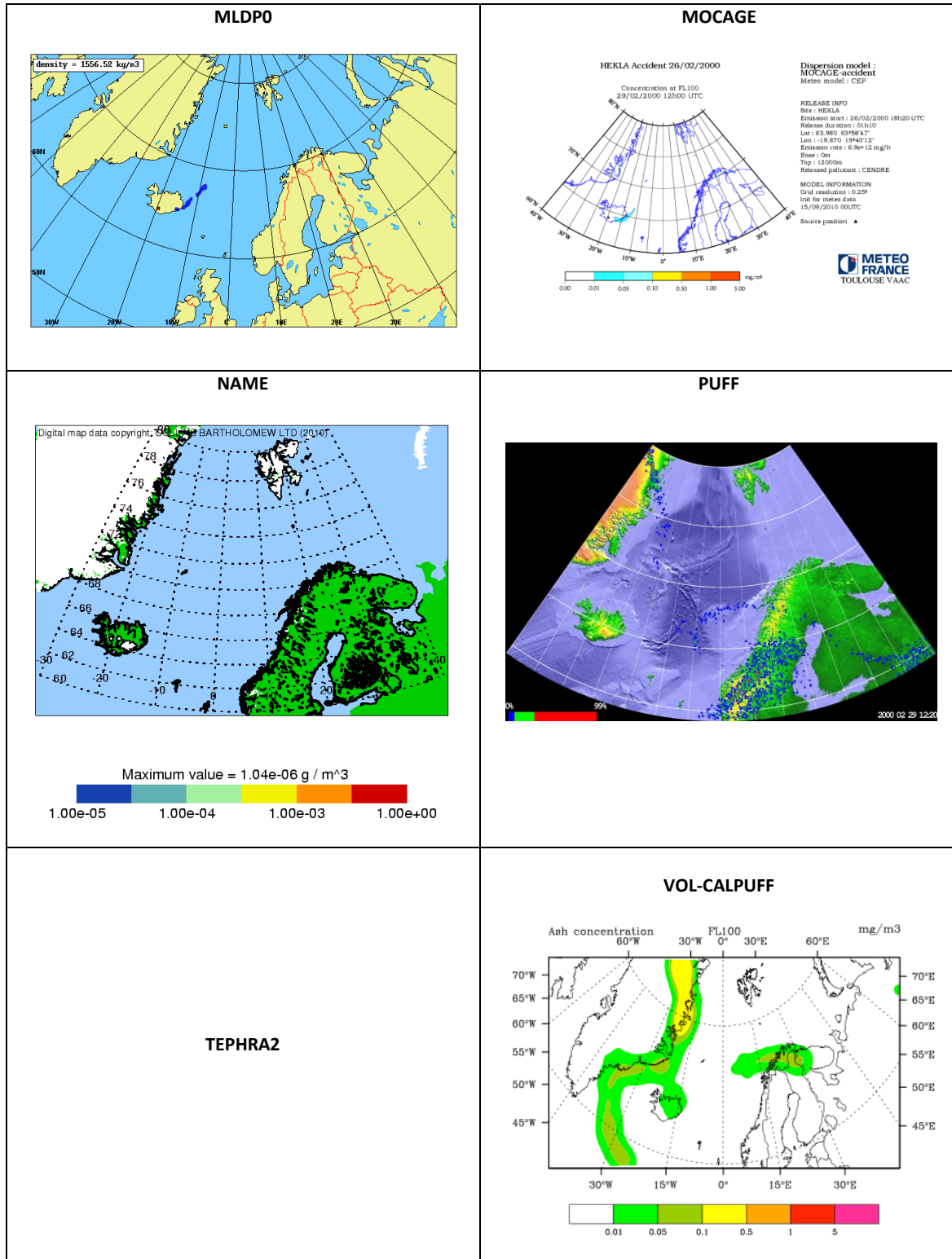




Plate 6.b

Concentration contours at FL200 (29 FEB 2000, 12:20UTC, 66h).

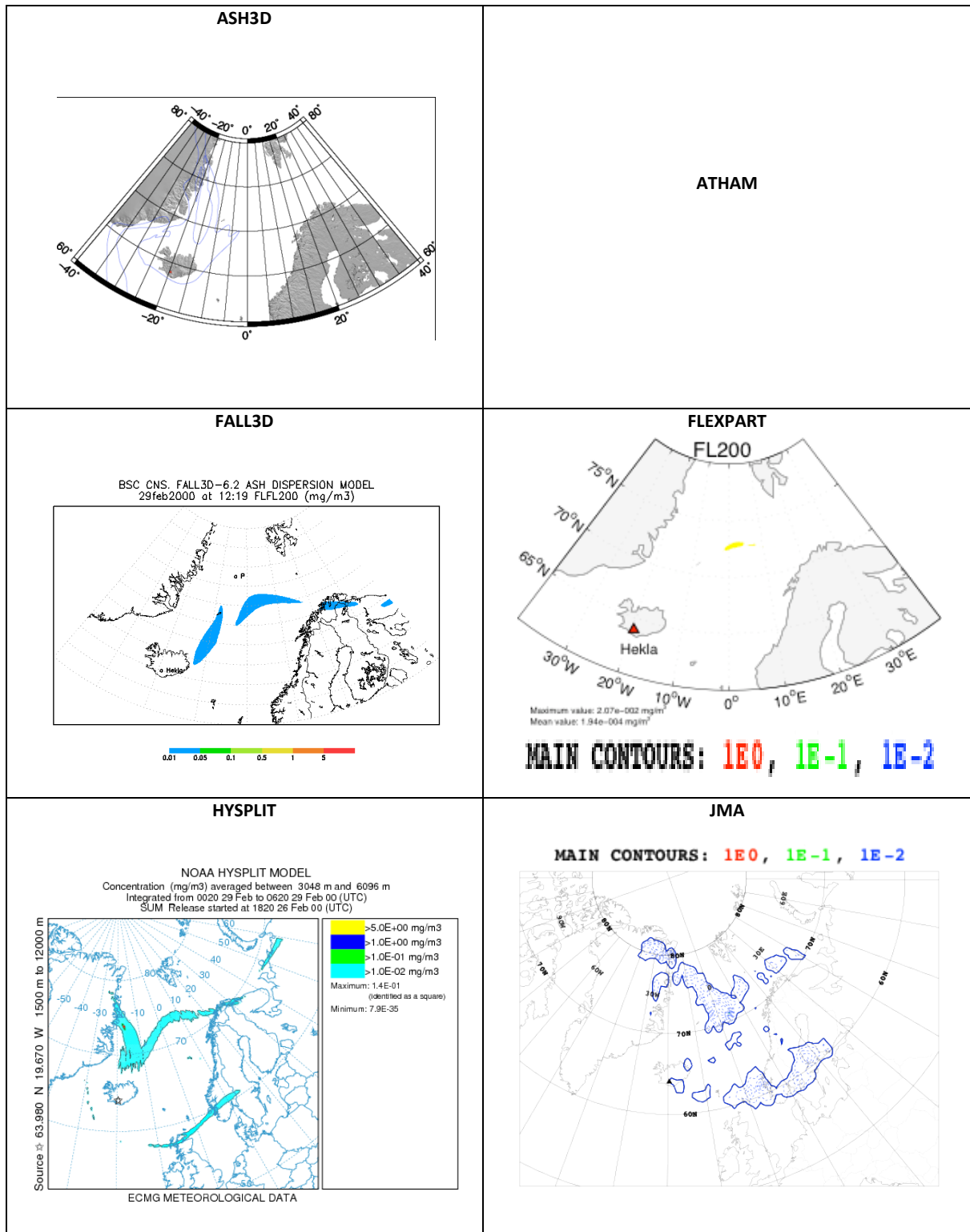




Plate 6.b (cont.)

Concentration contours at FL200 (29 FEB 2000, 12:20UTC, 66h).

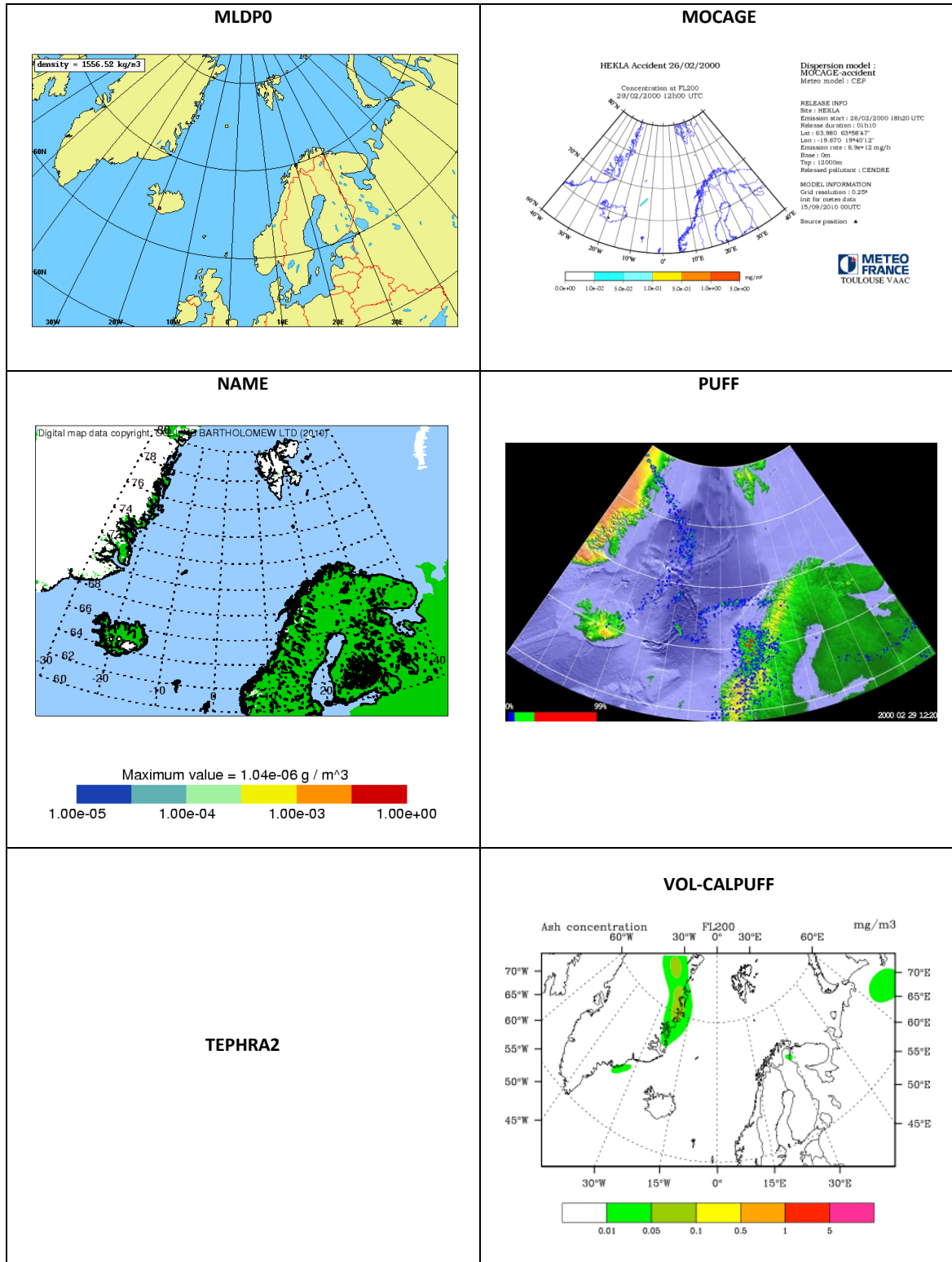




Plate 6.c

Concentration contours at FL300 (29 FEB 2000, 12:20UTC, 66h).

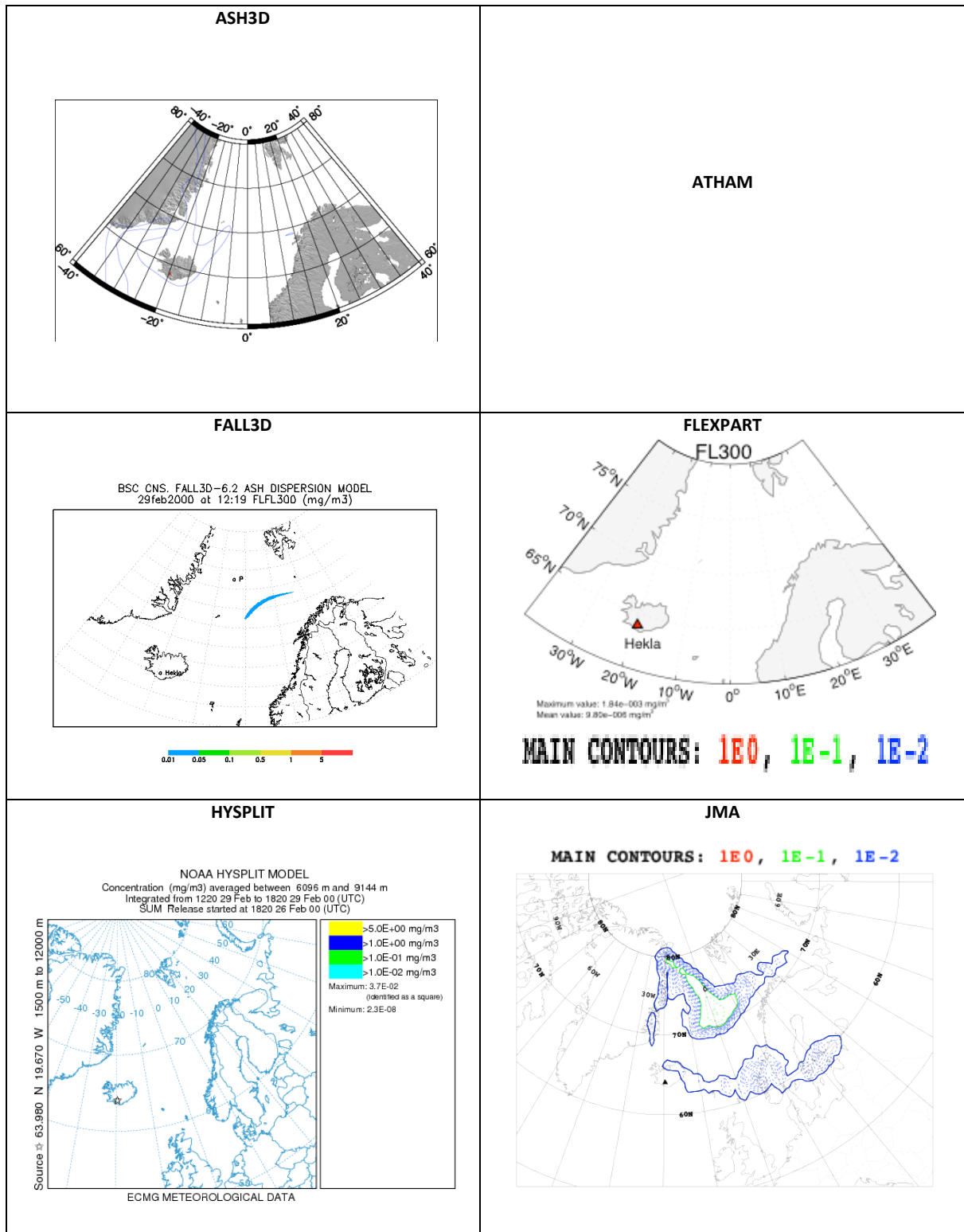




Plate 6.c (cont.)

Concentration contours at FL300 (29 FEB 2000, 12:20UTC, 66h).

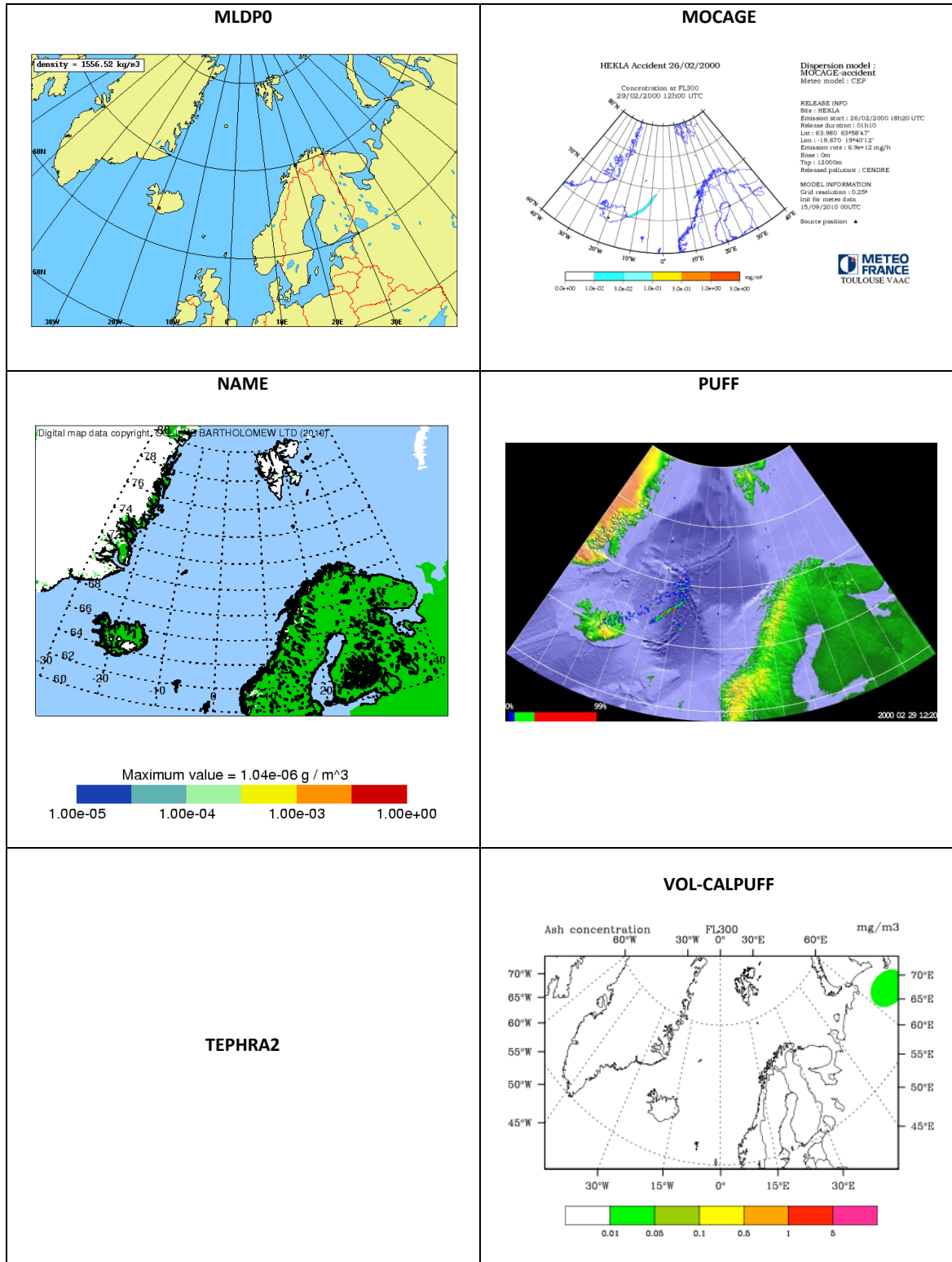


Plate 7.a

Vertical concentration profile (27 FEB 2000, 23:20UTC, 29h).

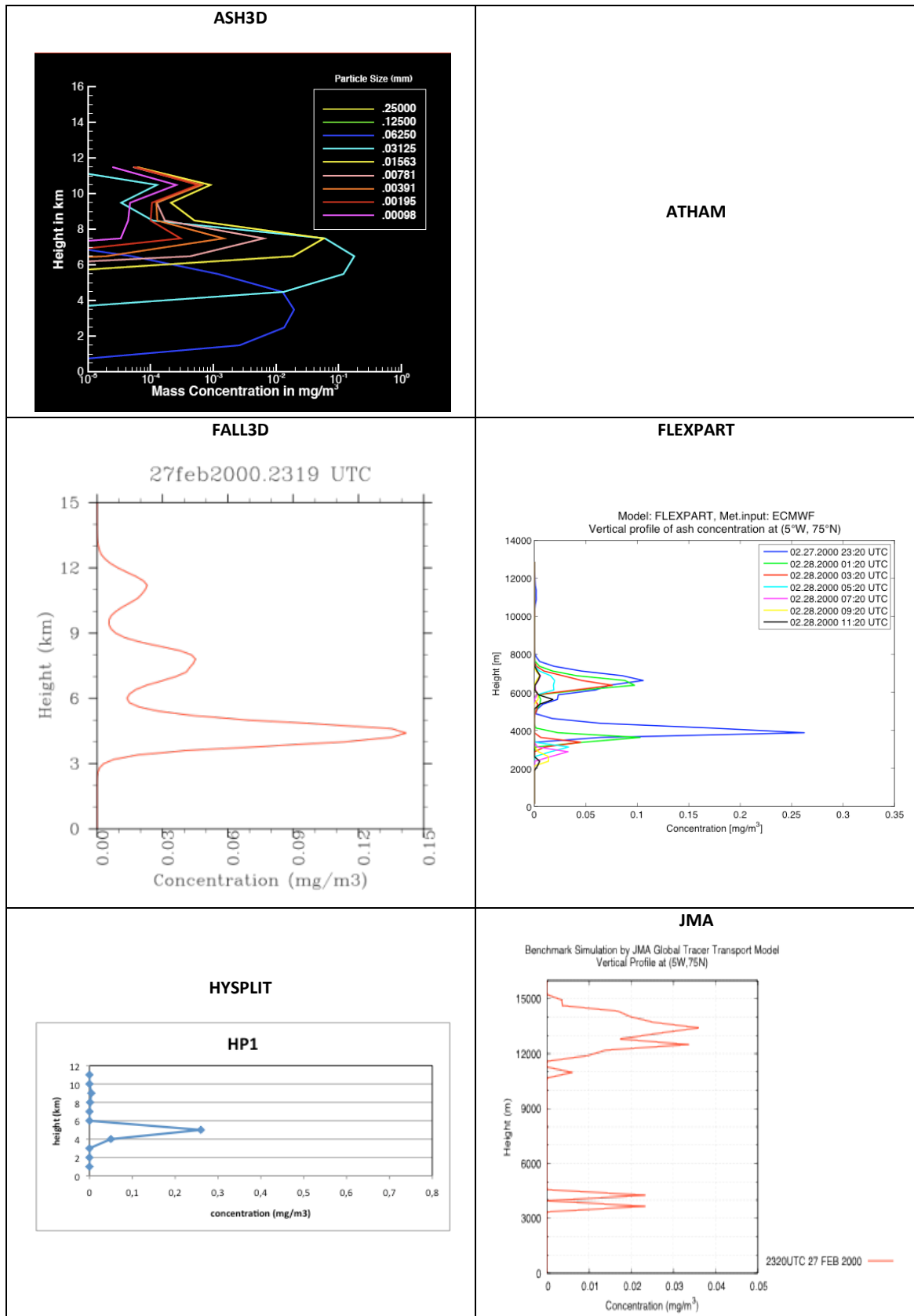




Plate 7.a (cont.)

Vertical concentration profile (27 FEB 2000, 23:20UTC, 29h).

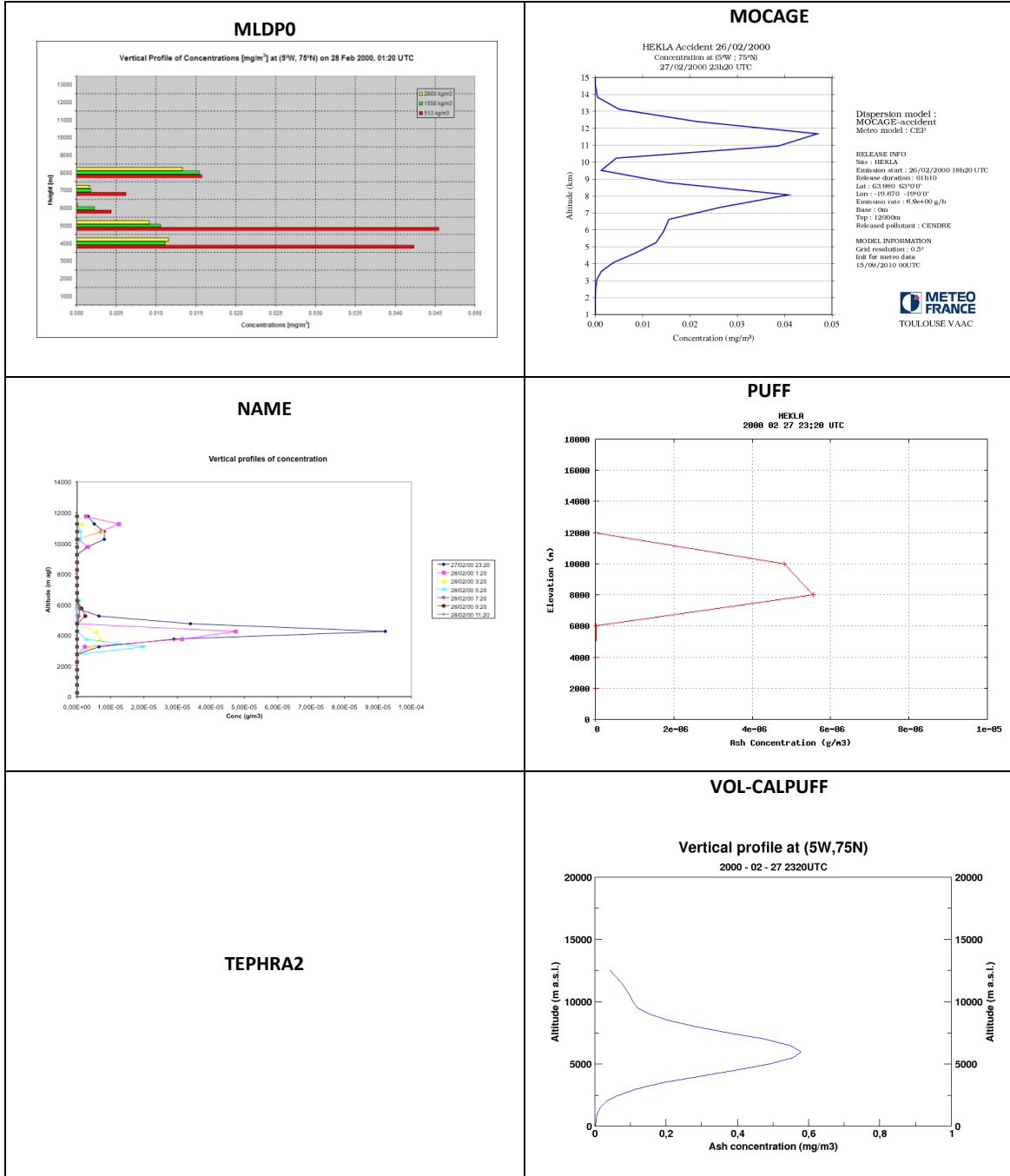


Plate 7.b

Vertical concentration profile (28 FEB 2000, 01:20UTC, 31h).

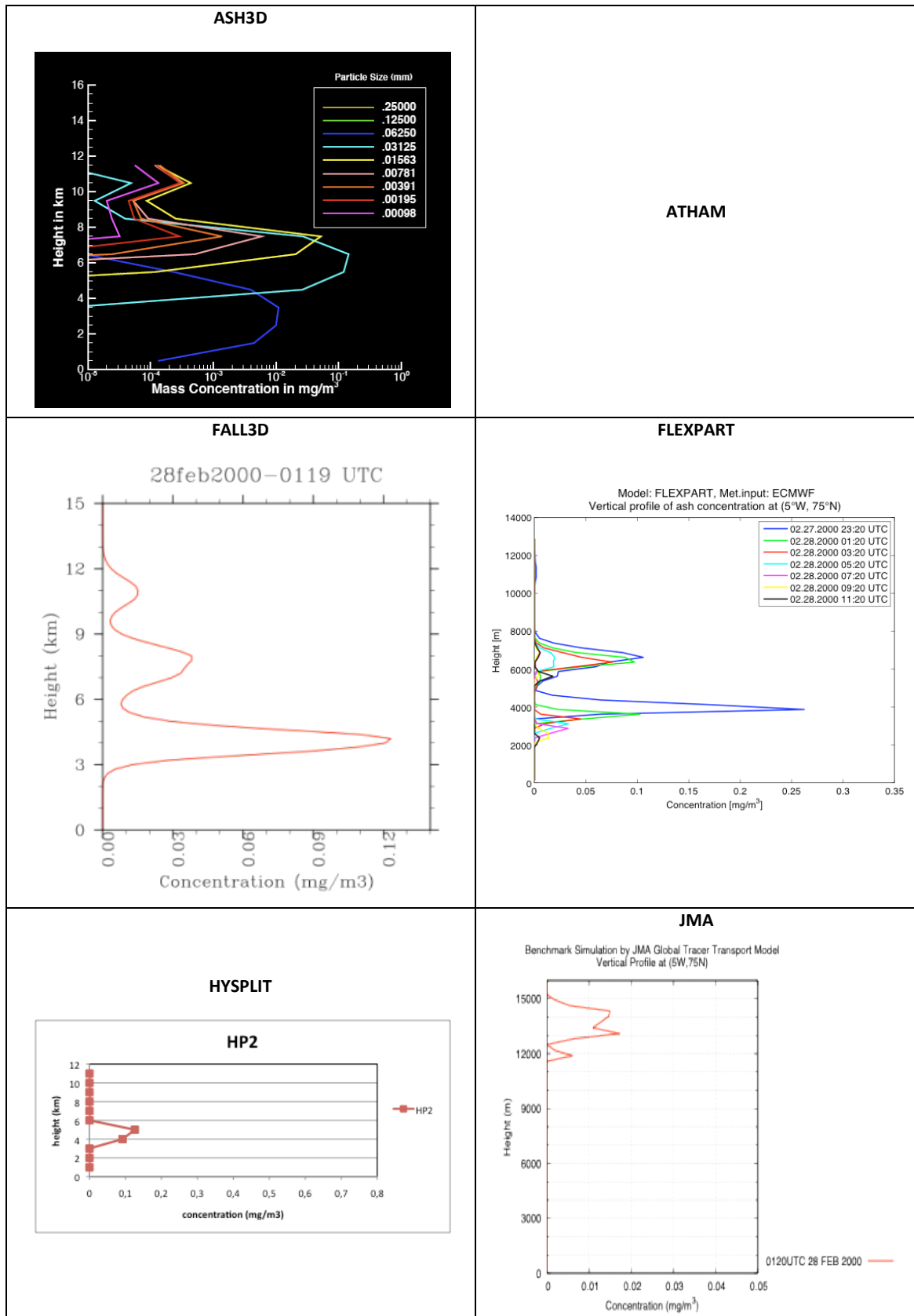


Plate 7.b (cont.)

Vertical concentration profile (28 FEB 2000, 01:20UTC, 31h).

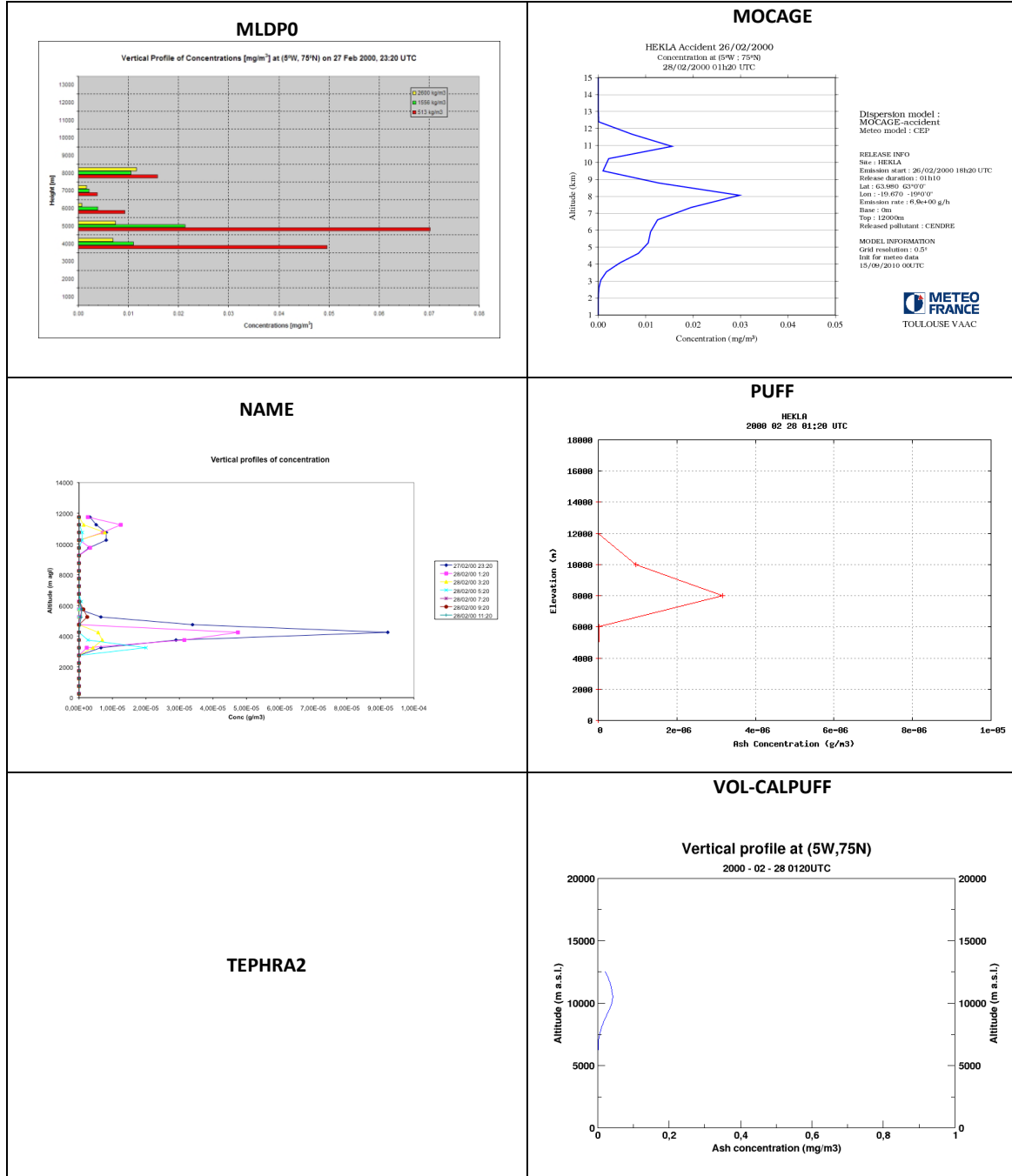


Plate 7.c

Vertical concentration profile (28 FEB 2000, 03:20UTC, 33h).

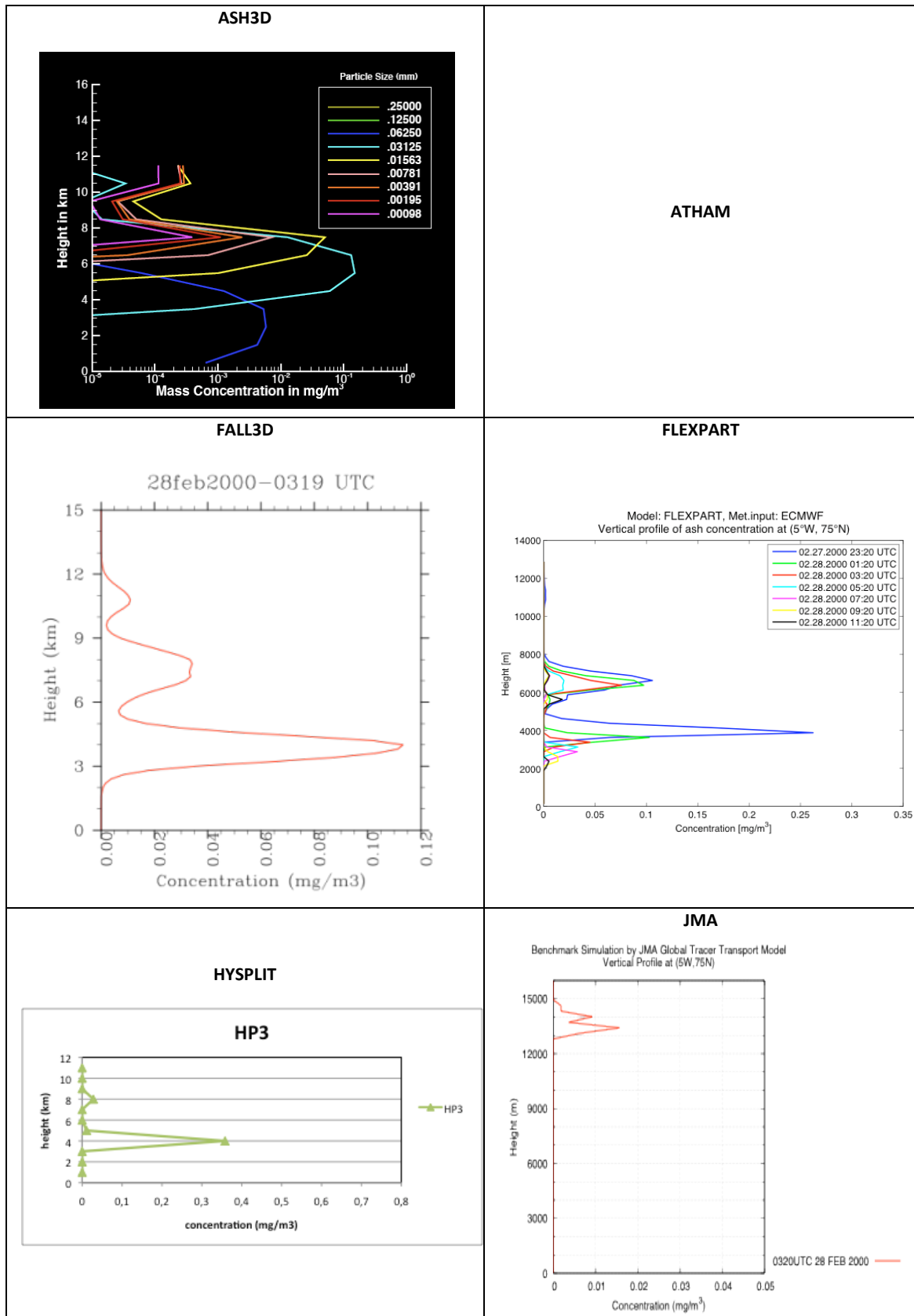




Plate 7.c (cont.)

Vertical concentration profile (28 FEB 2000, 03:20UTC, 33h).

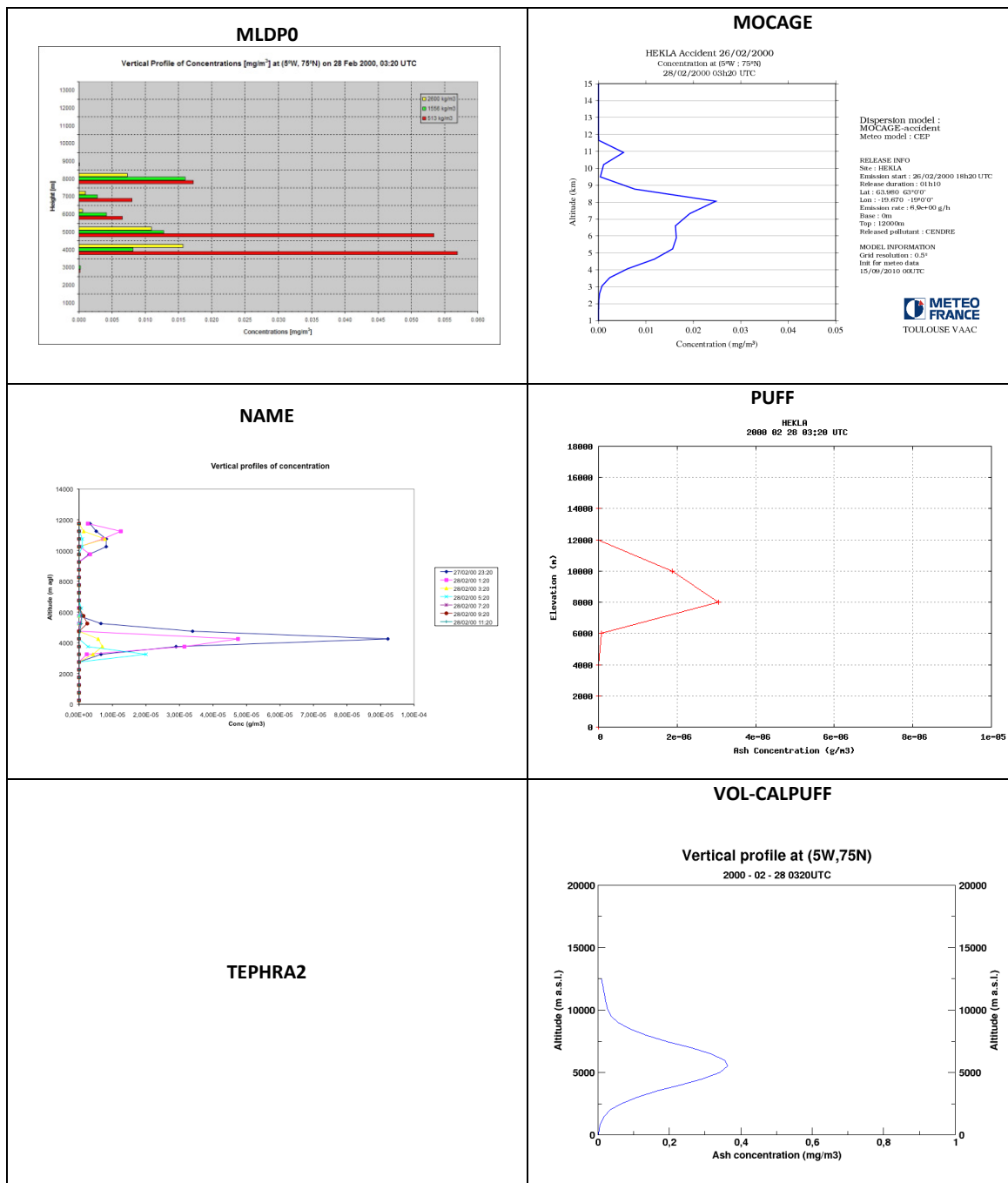


Plate 7.d

Vertical concentration profile (28 FEB 2000, 05:20UTC, 35h).

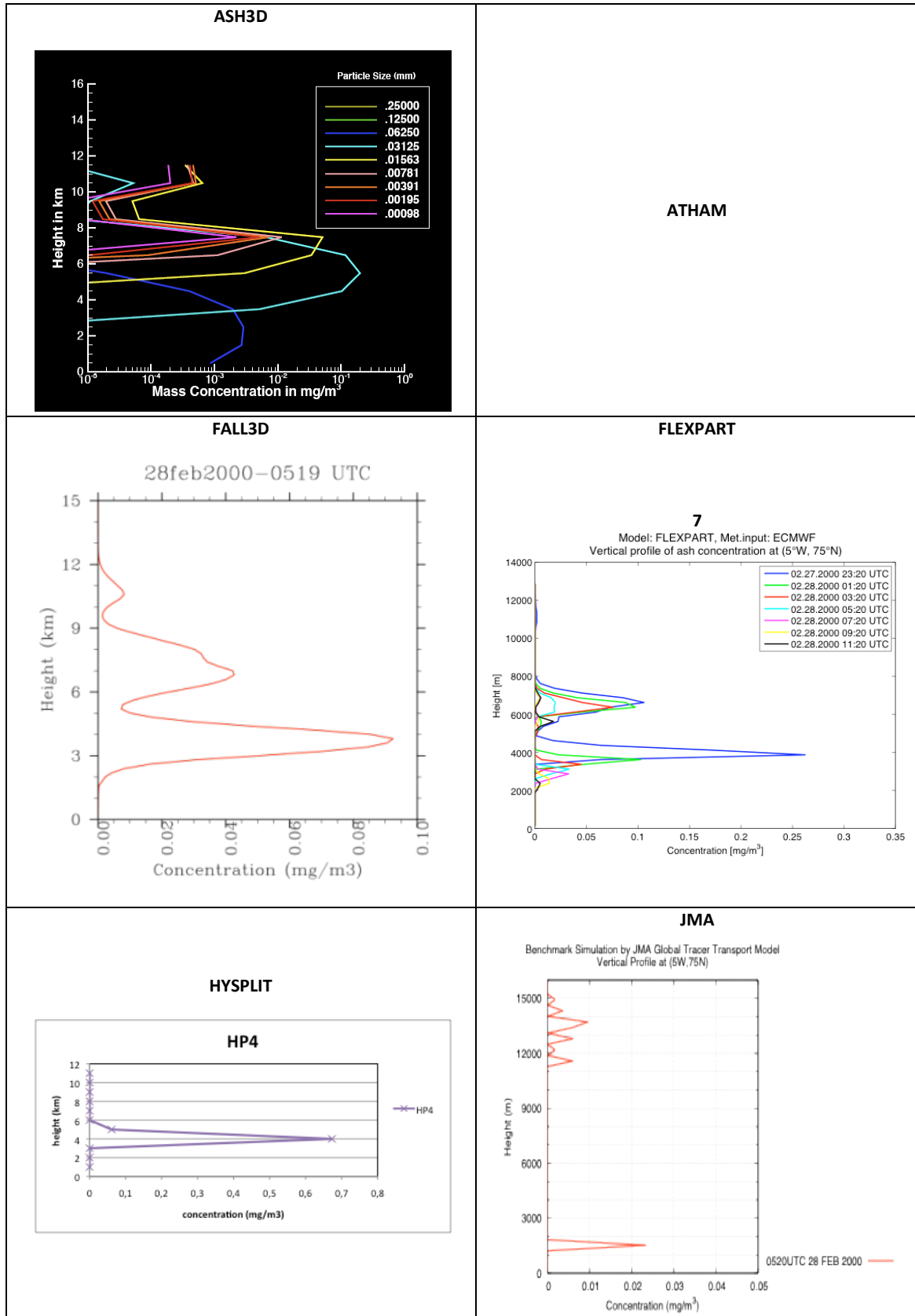




Plate 7.d (cont.)

Vertical concentration profile (28 FEB 2000, 05:20UTC, 35h).

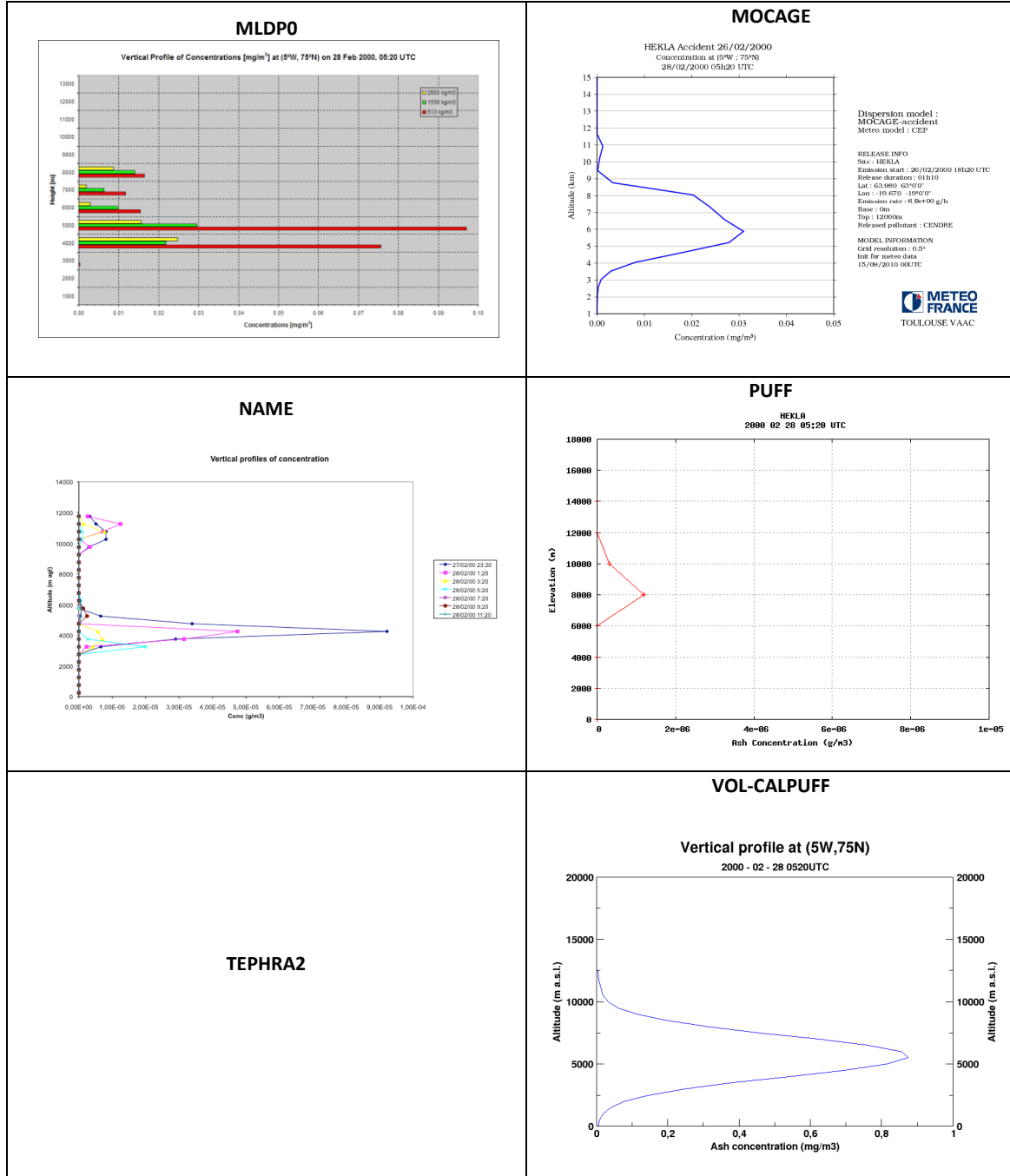


Plate 7.e

Vertical concentration profile (28 FEB 2000, 07:20UTC, 37h).

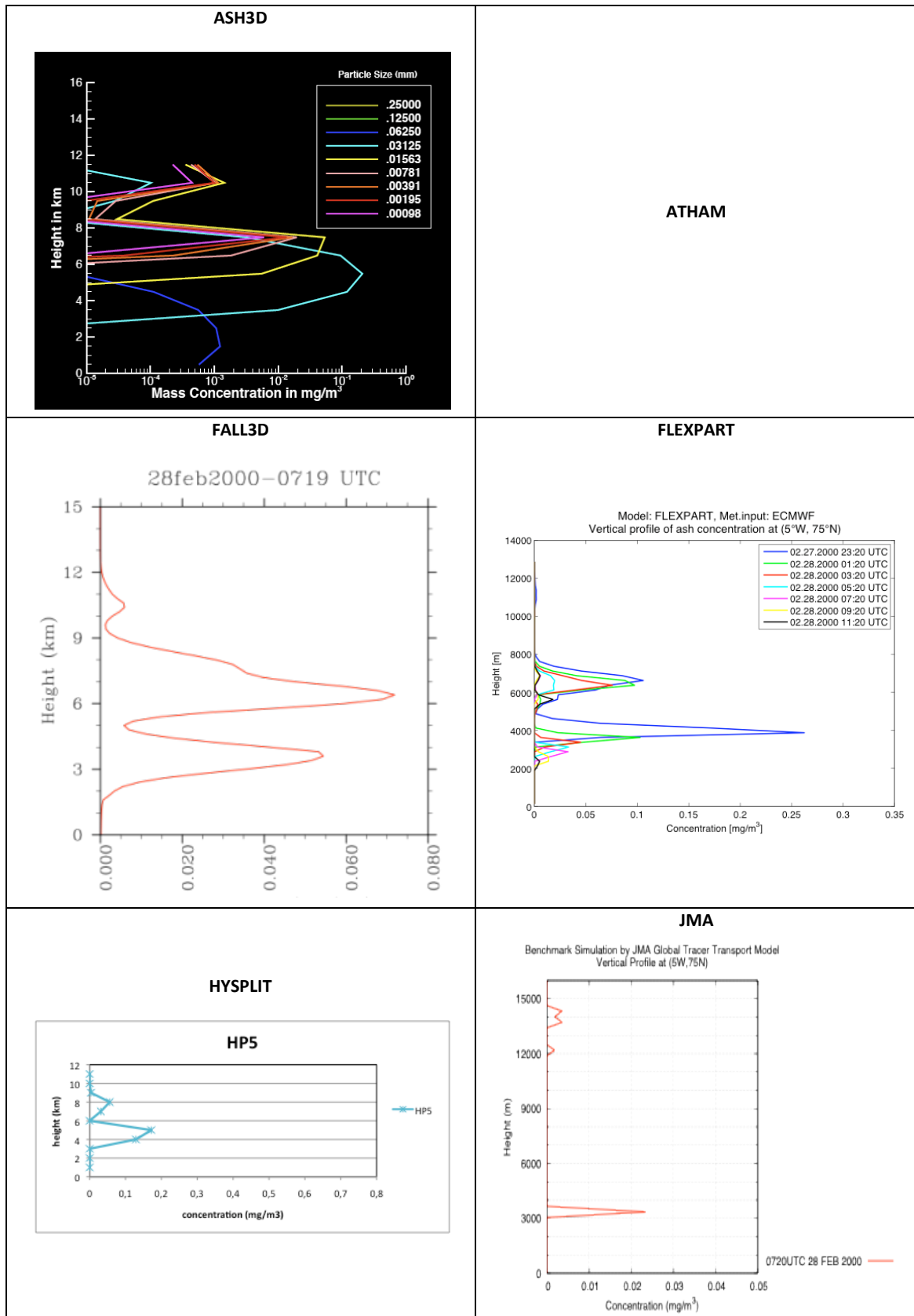




Plate 7.e (cont.)

Vertical concentration profile (28 FEB 2000, 07:20UTC, 37h).

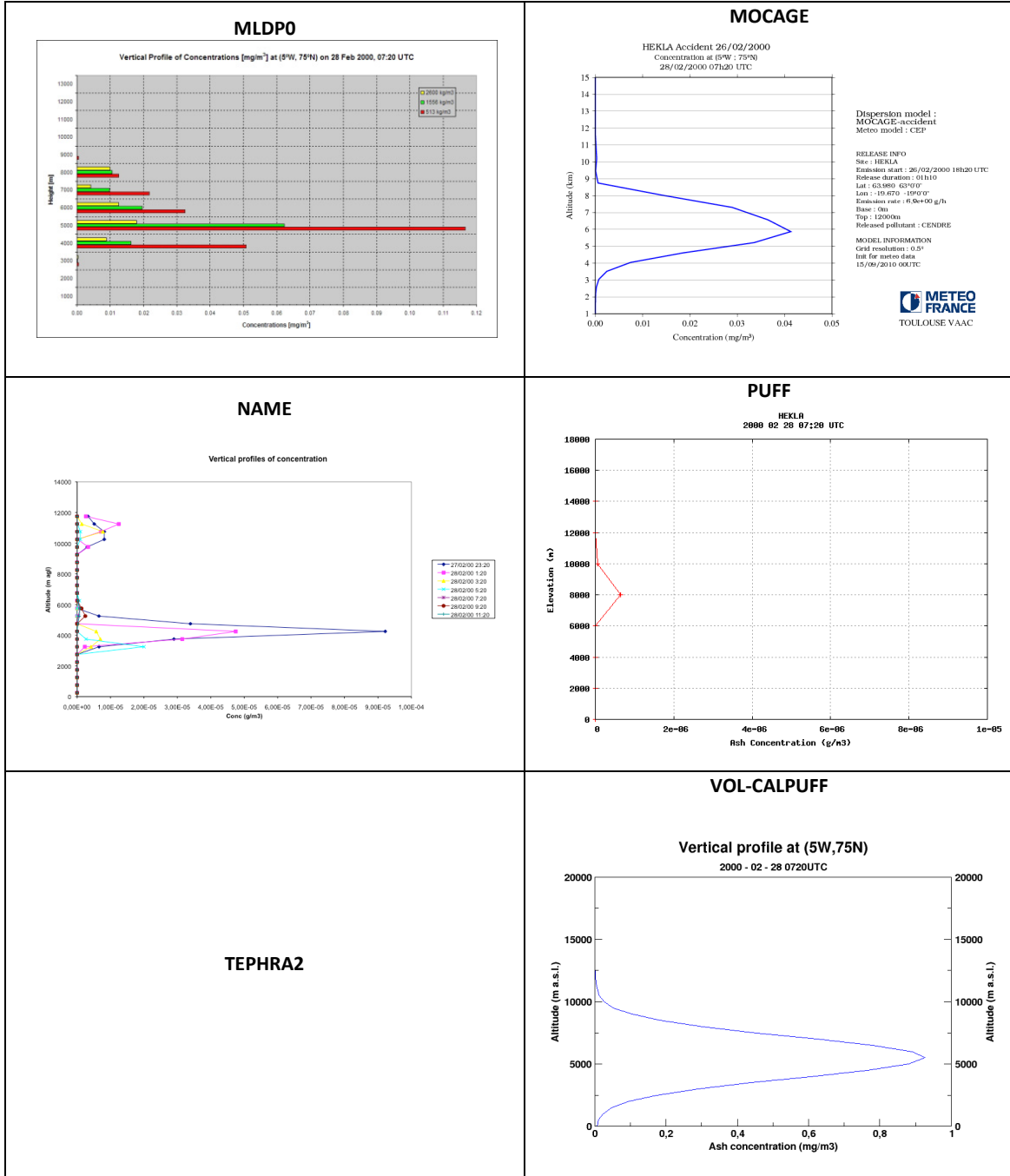


Plate 7.f

Vertical concentration profile (28 FEB 2000, 09:20UTC, 39h).

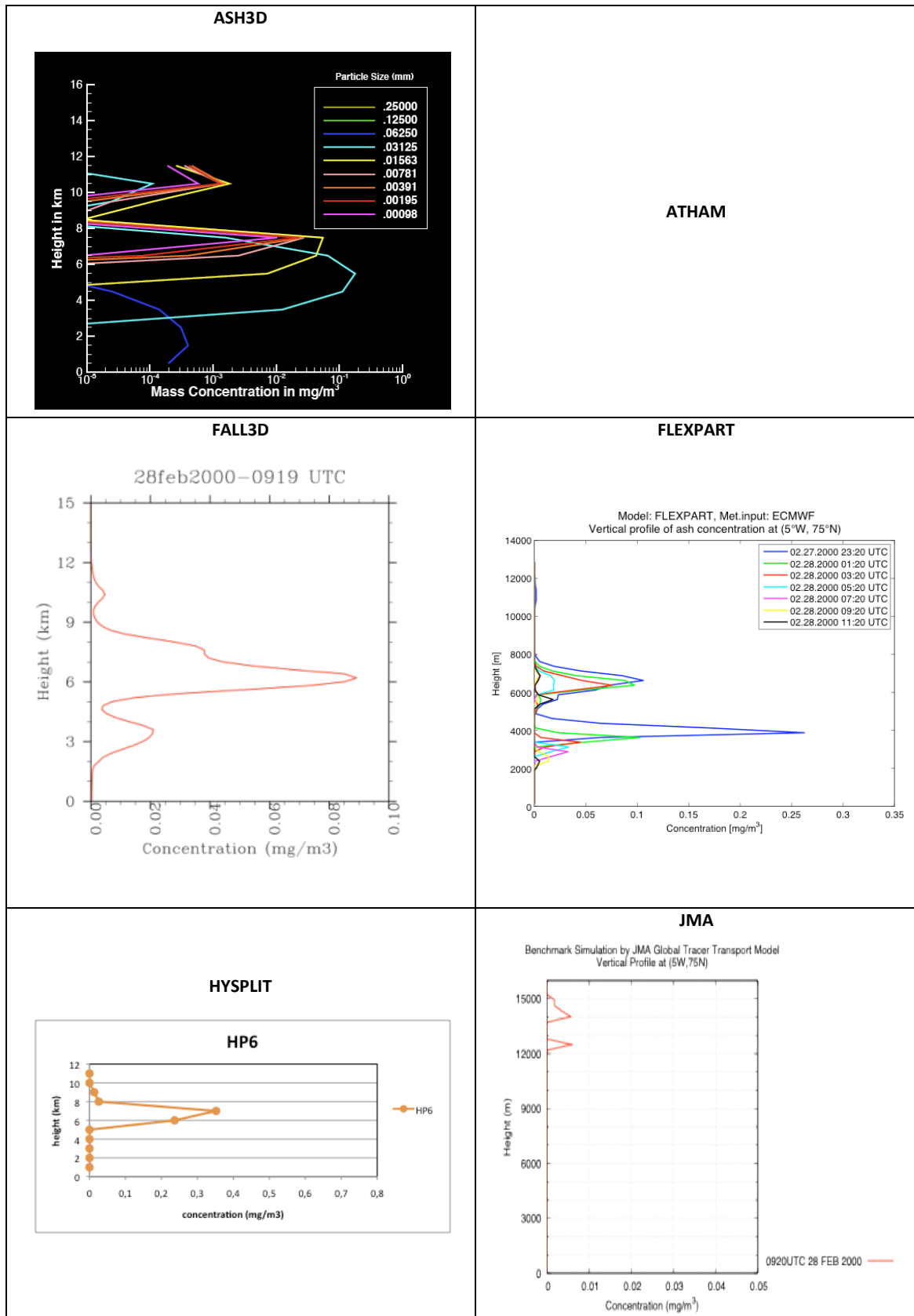




Plate 7.f (cont.)

Vertical concentration profile (28 FEB 2000, 09:20UTC, 39h).

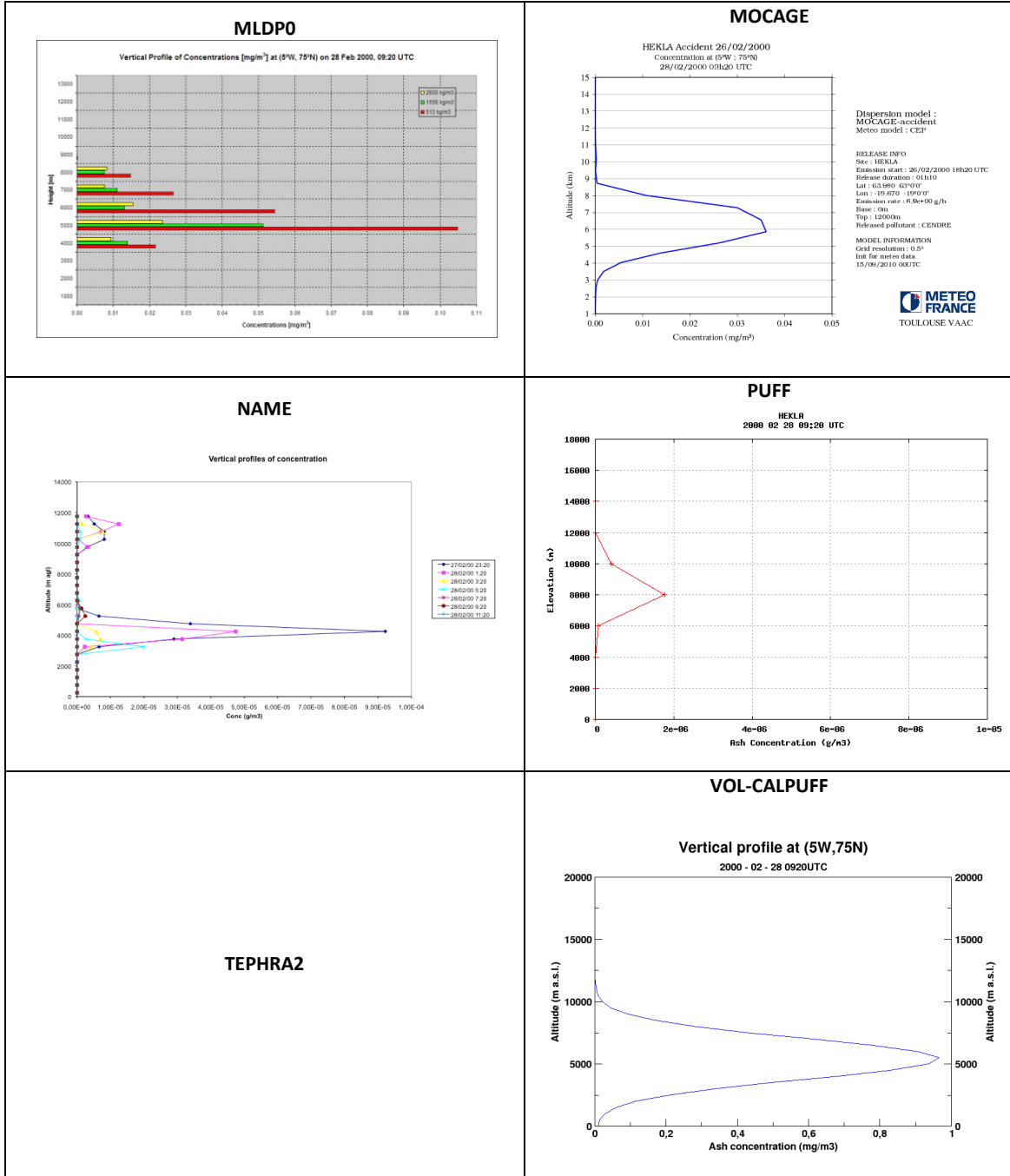


Plate 7.g
Vertical concentration profile (28 FEB 2000, 11:20UTC, 41h).

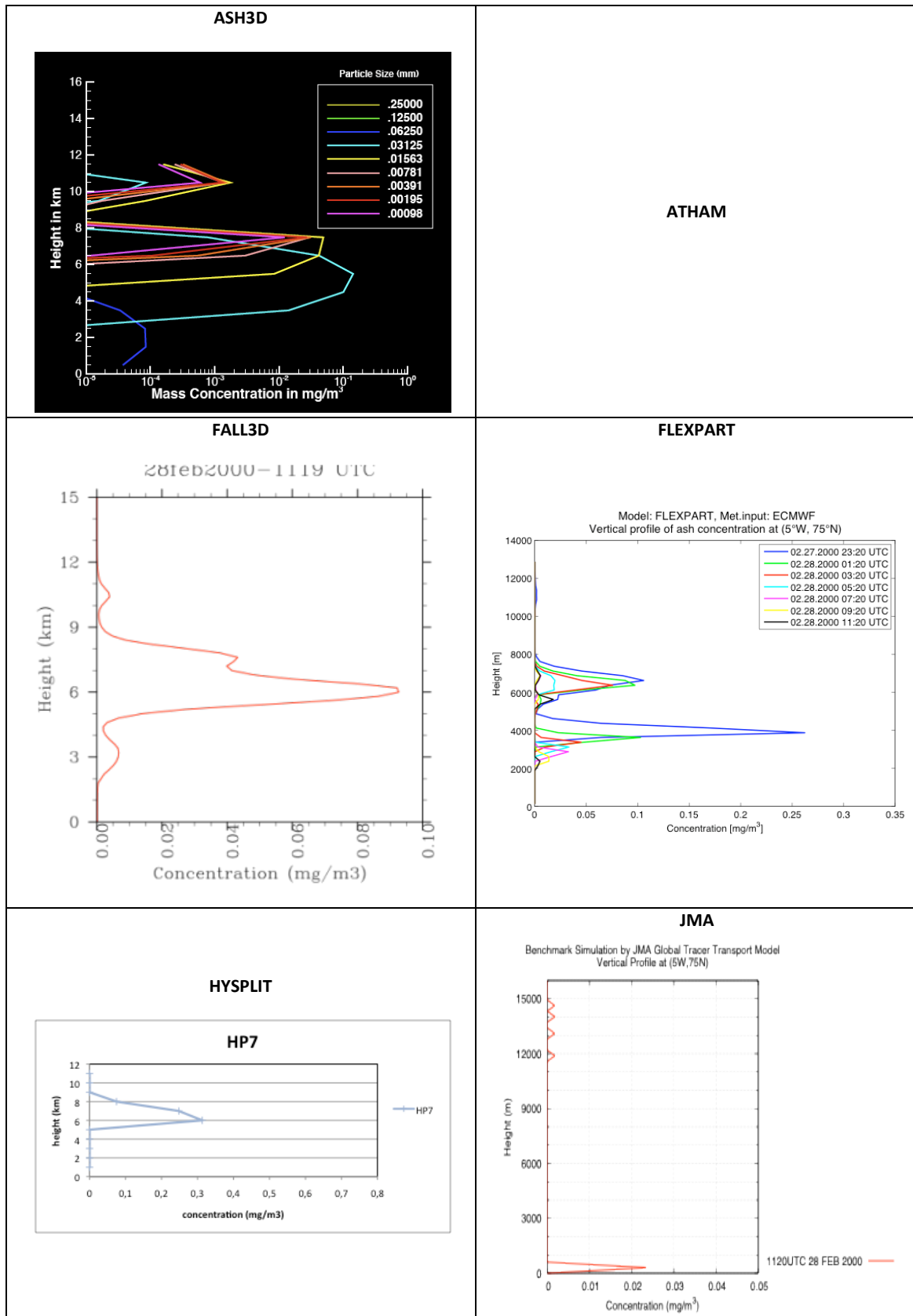




Plate 7.g (cont.)

Vertical concentration profile (28 FEB 2000, 11:20UTC, 41h).

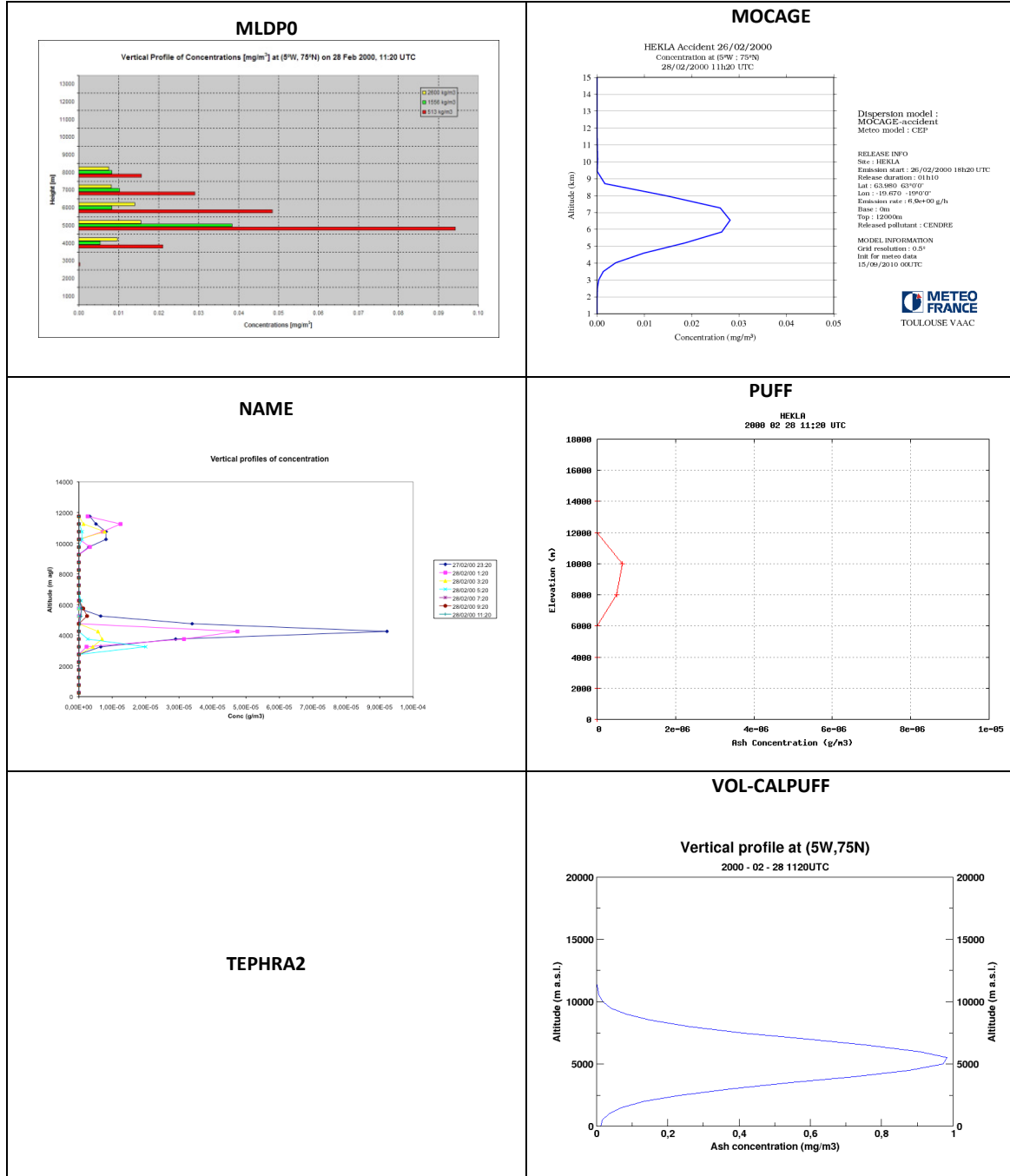


Plate 8.
Ground deposit load.

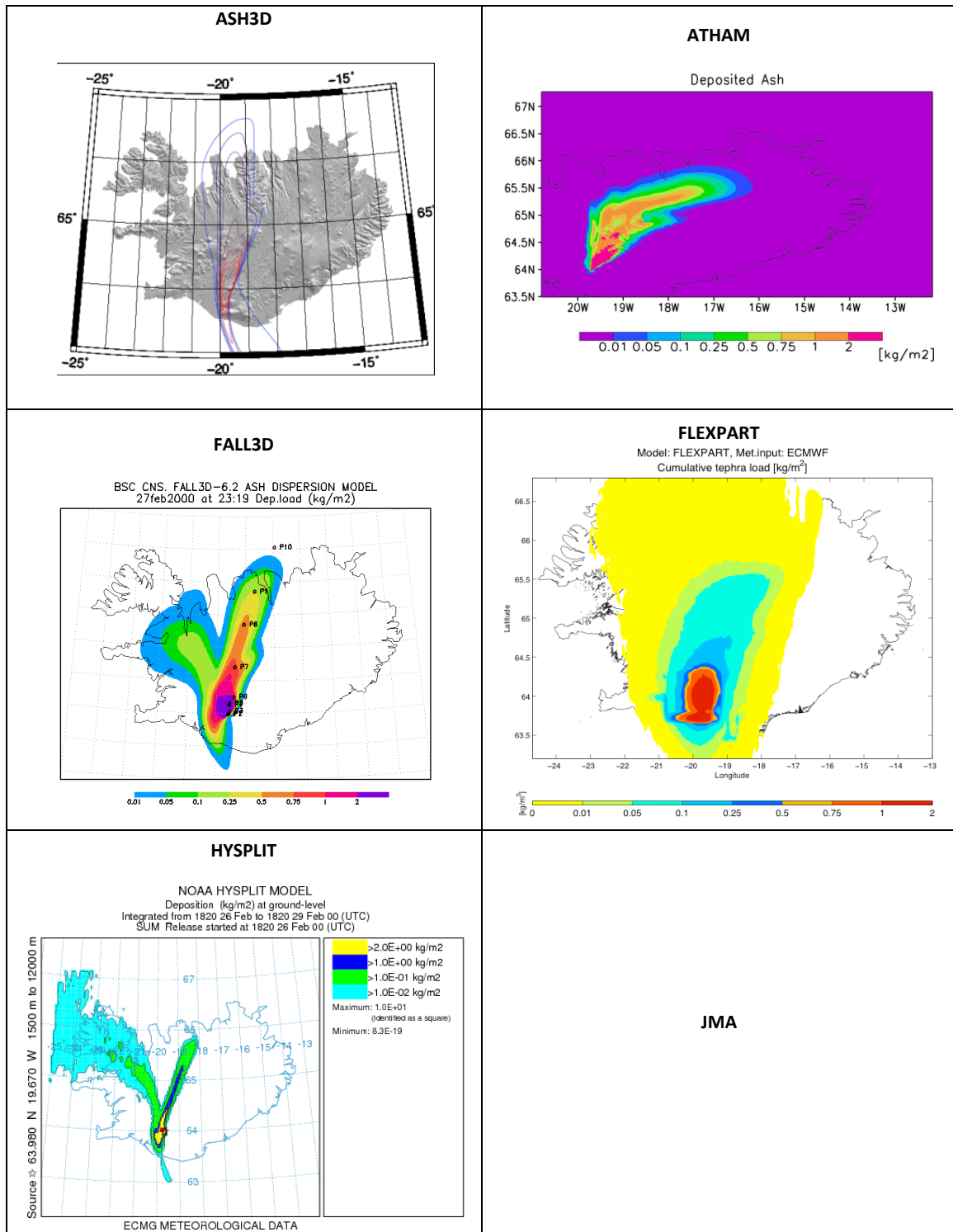
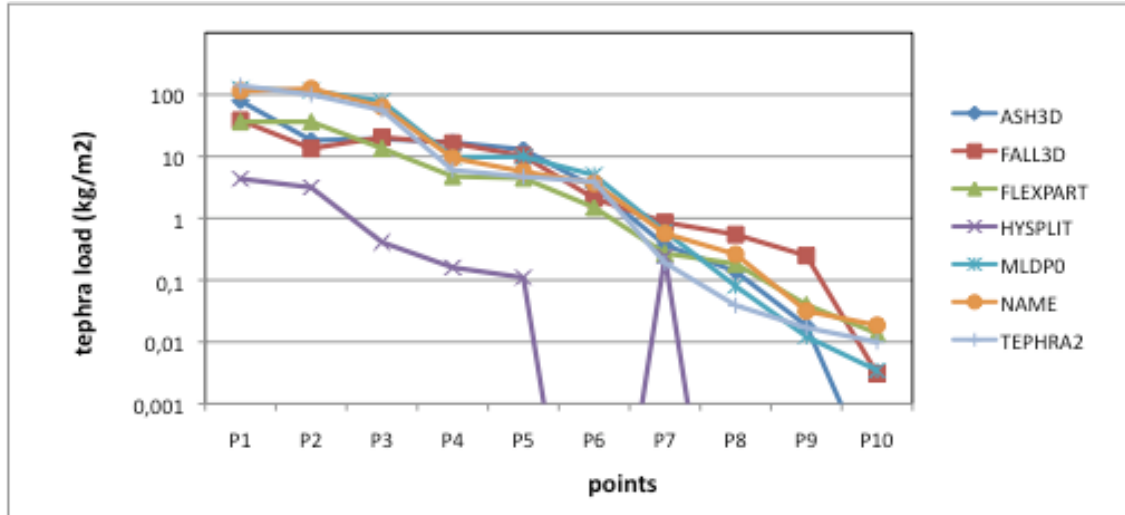


Plate 8 (cont).
Ground deposit load.

<p>MLDPO</p>	<p>MOCAGE</p>
<p>NAME</p>	<p>PUFF</p>
<p>TEPHRA2</p>	<p>VOL-CALPUFF</p>

Plate 9.

Ground deposit load at different distances from the vent.



UTM			
X (m)	Y (m)	Z (m)	Distance from source (km)
565532	7096993	1453	2.25
566435	7097879	1162	3.5
567915	7102424	485	7.84
566851	7112630	257	17.08
567586	7115674	258	20.19
574124	7126200	516	30.07
574247	7176994	588	81.77
587095	7249537	188	155.37
602785	7306504	135	214.05
633250	7382744	24	294.89